

Double exchange mechanisms for Mn doped III-V ferromagnetic semiconductors

P. M. Krstajić, F. M. Peeters

*Departement Natuurkunde, Universiteit Antwerpen (Campus Drie Eiken),
Universiteitsplein 1, B-2610 Antwerpen, Belgium*

V. A. Ivanov*

*N.S. Kurnakov Institute of the General and Inorganic
Chemistry of the Russian Academy of Sciences,
Leninskii prospect 31, 117 907 Moscow, Russia*

V. Fleurov#

*Raymond and Beverly Sackler Faculty of Exact Sciences,
School of Physics and Astronomy, Tel Aviv University,
Ramat Aviv, 69 978 Tel Aviv, Israel*

K. Kikoin

Physics Department, Ben-Gurion University, 84 105 Beer-Sheva, Israel

(Dated: May 28, 2018)

Abstract

A microscopic model of indirect exchange interaction between transition metal impurities in dilute magnetic semiconductors (DMS) is proposed. The hybridization of the impurity d-electrons with the heavy hole band states is largely responsible for the transfer of electrons between the impurities, whereas Hund rule for the electron occupation of the impurity d-shells makes the transfer spin selective. The model is applied to such systems as n -type GaN:Mn and p -type (Ga,Mn)As, p -type (Ga,Mn)P. In n -type DMS with $\text{Mn}^{2+}/3+$ impurities the exchange mechanisms is rather close to the kinematic exchange proposed by Zener for mixed-valence Mn ions. In p -type DMS ferromagnetism is governed by the kinematic mechanism involving the kinetic energy gain of heavy hole carriers caused by their hybridization with 3d electrons of Mn^{2+} impurities. Using the molecular field approximation the Curie temperatures T_C are calculated for several systems as functions of the impurity and hole concentrations. Comparison with the available experimental data shows a good agreement.

I. INTRODUCTION

Dilute magnetic semiconductors (DMS) are semiconductors, in which transition or rare-earth metal atoms randomly replace a fraction of atoms in one sublattice. Transition metal (TM) impurities, due to their high abundance and diffusivity, can easily enter the host semiconductor. In the group IV elemental semiconductors, they occupy mainly interstitial positions, whereas in III-V semiconductors the 3d TM impurities usually substitute group III atoms. The metastability of the zinc blende phase of the DMS (III,Mn)V compounds and low solubility of manganese in these materials were the major obstacles for a synthesis of dilute magnetic semiconductors.¹ However, the idea to combine in DMS the charge degrees of freedom of hole or electron carriers with the spin degrees of freedom of magnetic impurities became reality after a new doping technique based on non-equilibrium low temperature molecular beam epitaxy (LT-MBE)^{2,3} was developed. The discovery⁴ of ferromagnetic ordering in manganese doped InAs with the $T_C = 7.5\text{K}$ Curie temperature fuelled DMS studies that resulted in fabrication of (Ga,Mn)As compounds with $T_C = 110\text{K}$ ^{2,5} or even $T_C = 140\text{K}$.⁶ More recently^{7,8,9} Curie temperatures exceeding 150K were reported in (Ga,Mn)As. An above room temperature ferromagnetism was announced^{10,11} also in GaN and *p*-type GaP doped with Mn. Advanced III-V growth technique such as metal organic vapor phase epitaxy (MOVPE), or metal organic chemical vapor deposition (MOCVD) together with LT-MBE can produce good quality DMS with various element combinations.

A unique coexistence of high-temperature magnetism and semiconductor properties opens new venues of fundamental studies and applications of DMS's. The DMS's may be quite promising in spintronics, information technology,^{3,12} quantum computing,¹³ in manipulation of magnetism by an electric field¹⁴ and/or by illumination,¹⁵ in devices governed by the giant magnetoresistance effect,¹⁶ where the interlayer tunneling resistance is changed under the action of a magnetic field. Among the variety of applications one cannot exclude other functionalities such as nanostructure aspect of DMS:¹⁷ the DMS based quantum wells are expected to have unusual ferromagnetic properties with T_C (as shown in field effect transistors¹⁸) and high coercitivities¹⁹ tunable electrically, rather than magnetically.²⁰

Although ferromagnetic order in (Ga,Mn)As has been observed for the first time as early as²¹ 1996 with $T_C = 60\text{K}$, its microscopic origin from the theoretical point of view still remains not well understood. Extrapolating from (Ga,Mn)As, FM ordering with high T_C was predicted for *p*-type (Ga,Mn)N²² and found in Ref. 11. However, a direct extrapolation of the trends known for the GaAs-based material characterized by a relatively narrow forbidden energy gap to the wide gap GaN DMS is not well founded. The differences in formation of the ferromagnetic order arise from the differences in the structure of chemical bonds between the Mn impurity and valence electrons in various III-V host semiconductors. The purpose of the present paper is to pinpoint these differences and to construct a general microscopic theory of the double exchange (superexchange) in dilute magnetic semiconductors.

There are three approaches, which one may follow to study magnetic states of DMS's. According to the first approach, one chooses an effective spin Hamiltonian and calculates

the corresponding exchange coupling constant in the course of this derivation. The major part of the available descriptions of the FM order in such DMS's as (Ga,Mn)As, (Ga,Mn)P and (Ga,Mn)N, are based on semi-phenomenological models, which postulate the existence of local magnetic moments on the Mn sites, as well as an indirect exchange between these moments and the electrons in the valence band of the host semiconductor.^{17,23,24,25,26} Some of these theories emphasize the role of shallow acceptor levels existing in the first two of these systems²⁷ or of resonance levels.²⁸

The second approach is based on an extended cluster method, where a cubic supercell with a magnetic Mn ion in its center is used to calculate the density of spin polarized states of a "homogeneously doped" crystal (see e.g., Refs. 29,30). The resulting picture provides information about positions and occupation of Mn-related majority and minority "bands". Sometimes an effective $s - d$ exchange Hamiltonian is introduced phenomenologically in this picture, and the effective exchange constant is chosen to fit the numerical data (see Ref. 29 and the first paper in Ref. 30).

According to the third approach, realistic exchange parameters should be derived within the framework of a microscopic theory based on the knowledge of the electronic structure of III-V semiconductors doped with TM impurities. An exhaustive microscopic theory for isolated TM impurities in semiconductors was constructed more than two decades ago starting with the papers of Refs. 31,32 (see monograph Ref. 33 for a detailed description and Ref. 34 where a powerful numeric approach was developed). This theory contains all necessary ingredients for an accurate derivation of the indirect magnetic exchange between interacting impurities. Our first attempt³⁵ to apply this theory to (Ga,Mn)As resulted in a quantitative description of the hole concentration dependent Curie temperature T_C in p -type DMS's within the framework of a very simple model Hamiltonian, in which the effective *kinematic exchange* results from hopping between the occupied d -states of the half-filled d -shell of the Mn impurity via empty heavy hole (hh) states near the top of the valence band.

Here we present a general theory of the double exchange interaction in Mn-doped III-V semiconductors, which covers both p - and n -type materials. The theory establishes differences between the exchange mechanisms in these two cases and demonstrates that the conventional Zener double exchange mechanism³⁶ is realized only in n -type DMS (presumably, in (Ga,Mn)N).

It is well known that the TM ions may introduce impurity levels in the forbidden energy gap. Among them the manganese impurity in GaAs and some other semiconductors exhibit peculiar features. According to its position in the series of the TM elements, a neutral impurity Mn^{3+} in the Ga-site is expected to have the $3d^4$ configuration. However, the Mn ion retains its fifth electron in its $3d$ shell, because of an exceptional stability of the high-spin half-filled $3d^5$ state resulting from the strong intra-atomic Hund interaction. The manganese impurities not only introduce magnetic moments in the p -type (III,Mn)V compounds but also create potentials attracting holes, i.e. act as acceptors. Therefore, the neutral substitution impurity state is $A^0(3d^5\bar{p})$, where \bar{p} stands for the loosely bound hole, and the manganese provides both holes and magnetic moments to the host, A is the spectroscopic notation indicating the irreducible representation describing this state (more about these notations can be found, e.g. in Ref. 33)

Existence of the complex $\text{Mn } d^5\bar{p}$ in lightly doped bulk GaAs is detected by electron spin resonance measurements³⁷ and by infrared spectroscopy.³⁸ These studies discovered an acceptor level inside the energy gap around 110 meV above the top of the valence band. This value is substantially higher than 30 meV resulting from conventional effective mass theory,³⁷ which already implies that treatment of the manganese impurities in III-V compounds requires a more refined approach. On the other hand, the presence of negatively ionized complexes $A^-(3d^5)$ is detected in (Ga,Mn)As epilayers grown by low temperature molecular beam epitaxy,³⁹ which indicates that both mobile and localized holes exist in ferromagnetic (Ga,Mn)As. The coexistence of weakly and strongly localized states is also in accordance with *ac* conductivity experiments.⁴⁰

Apparently, a similar impurity electronic structure is realized in (Ga,Mn)P. But in contrast, Mn in the wide gap GaN semiconductor releases one of its *d*-electrons to the valence band, which is typical of all other TM impurities, and remains in the $\text{Mn}^{3+}(d^4)$ state, unless the sample is deliberately *n*-doped. The latter state is neutral, so there is no need in binding a hole to maintain the neutrality of the ground state. This leaves no room for a direct extrapolation from (Ga,Mn)As to (Ga,Mn)N, and the kinematic inter-impurity exchange mechanisms in these two systems should be considered separately.

In this paper we will develop a general theory of ferromagnetic exchange in DMS's. It turns out that the Zener mechanism³⁶ in its classical form is realized in *n*-type (Ga,Mn)N, whereas the *p*-type systems (Ga,Mn)As, (Ga,Mn)P and, possibly, *p*-(Ga,Mn)N are examples of another type of indirect (kinematic) exchange interaction, which was not observed in the family of Mn oxides described by the Zener theory of ferromagnetic insulators. The paper is organized as follows. Section II presents a detailed description of the microscopic model including the calculation of the exchange interaction between TM impurities. Since this calculation appears to be rather involved, its mathematical details are given in the Appendix. In Section III we apply the results obtained in Section II to *p*-type semiconductors, find the kinematic exchange interaction and using the molecular field approximation calculate the Curie temperature as a function of the Mn content and hole concentration for *p*-type (Ga,Mn)As and (Ga,Mn)P. The results are compared with available experimental data. The *n*-type (Ga,Mn)N DMS's, which possesses specific features differing it from other DMS's, is discussed in Section IV. Finally, the scope of the theory and comparison with other approaches are summarized in the concluding Section V.

II. INDIRECT EXCHANGE INTERACTION BETWEEN TWO MAGNETIC IMPURITIES

According to the general principles of the theory of isolated TM in semiconductors,^{33,34} the electronic spectrum of these impurities in III-V semiconductors is predetermined by the structure of chemical bonds (hybridization) between the *3d*-orbitals of impurity ions and the *p*-orbitals of the valence band electrons, whereas their magnetic state is governed by the Coulomb and exchange interactions within the *3d*-atomic shell (intra-atomic electron-electron correlations), modified by hybridization with the electron states of the crystalline environment.

The localized TM impurity d -states possess t_2 and e symmetry of the crystal point symmetry group T_d as revealed in the theoretical studies of electronic properties of isolated TM impurities in semiconductors carried out in the 70's and 80's (see, e.g. Refs. 41, 42,43,44,45). The e states are practically nonbonding d -states of the impurity $3d$ shell, whereas the t_2 states form bonding and antibonding configurations with the p -states of the valence band. The two latter types of states are classified as the crystal field resonances (CFR), in which the d -component dominates, and the dangling bond hybrids (DBH) with predominantly p -type contribution of the valence band states. Crucially important is that the absolute positions of CFR levels relatively weakly depend on the band structure of the host semiconductor material. The CFR levels are pinned mainly to the vacuum energy, and this pinning is modulated by the counterbalanced interactions with valence and conduction band states.^{33,46} The DBH states are more intimately connected with the peak in the density of states of the heavy hole band, which dominates the pd -hybridization. The variety of electronic and magnetic properties of Mn and other TM ions in different III-V host semiconductors stems from these universal chemical trends.

Due to a large mismatch between positions of the valence bands in GaAs, GaP on the one side and in GaN on the other side, the Mn(d^5/d^4) CFR level falls deep in the valence band in GaAs, GaP and appears within the forbidden energy gap of GaN. The CFR nature of Mn (d^5/d^4) t_2 -level near the middle of the gap for (Ga,Mn)N is confirmed experimentally⁴⁷ and follows also from numerical calculations.³⁰ This t_2 -level is *empty* in the neutral state Mn³⁺(d^4) of the substitution impurity. It becomes magnetically active only in n doped materials, e.g. in (Ga,Mn)N, where part of the Mn impurities capture donor electrons and transform into charged ions Mn²⁺(d^5). A similar behavior is characteristic of all other light TM ions in all III-V compounds including GaAs and GaP.^{33,34,42}

Since the position of the valence band in GaAs and GaP is substantially higher in the absolute energy scale (with the vacuum energy as the reference point) than those in GaN, the CFR t_2 level (d^5/d^4) in the (Ga,Mn)As and (Ga,Mn)P DMS's falls below the center of gravity of the valence band. Therefore, this CFR level is always occupied, Mn ions retain their fifth electron in the $3d$ -shell, and the neutral substitution impurity state is ($3d^5\bar{p}$), where \bar{p} stands for a loosely bound hole occupying the relatively shallow acceptor level in the forbidden energy gap of GaAs and GaP semiconductors.

Both of the above mentioned situations may be described within the resonance scattering model of the TM impurity states in semiconductors based on the Anderson single impurity Hamiltonian, proposed originally for TM impurities in metals,⁴⁸ and later modified for semiconductors in Refs. 31,32,43,45,46. An extension of the Anderson model to two TM impurities in metals was proposed in Ref. 49 resulting in a ferromagnetic coupling in TM doped metals. Using this model Ref 50 derived an interaction similar to the RKKY interaction. Here we discuss a model describing interaction between Mn (and other TM) impurities in a semiconductor host. In accordance with Hund rule for the electron occupation in Mn ions in a tetrahedral environment,^{33,34,51} two competing states Mn(d^4) and Mn (d^5), involved in the double exchange in DMS, have the $d^4(e^2t^2)$ and $d^5(e^2t^3)$ configurations, respectively. The next charged state $d^6(e^3t^3)$ has a much higher energy due to the strong intra-ionic Coulomb interaction. Therefore, the 'passive' nonbonding

e -electrons may be excluded from our consideration. The indirect exchange between magnetic moments is mediated by virtual transitions of t_2 electrons into unoccupied valence band states.

The Hamiltonian for two TM impurities in a III-V semiconductor has the form:

$$H = H_h + H_d + H_{hd}, \quad (1)$$

where the band Hamiltonian

$$H_h = \sum_{\mathbf{p}, \sigma} \varepsilon_{\mathbf{p}}^h c_{\mathbf{p}h\sigma}^\dagger c_{\mathbf{p}h\sigma} \quad (2)$$

includes only the heavy hole band. Here $c_{\mathbf{p}h\sigma}^\dagger$ ($c_{\mathbf{p}h\sigma}$) is the creation (annihilation) operator of a hole with momentum \mathbf{p} and spin orientation σ in the hh band of the semiconductor with the energy dispersion $\varepsilon_{\mathbf{p}}^h$. The heavy hole band gives the dominant contribution to the formation of the impurity states,^{33,34} and governs the onset of ferromagnetic order. The second term in the Hamiltonian (1) describes the electrons within the Mn atoms with a possible account of the crystal field of the surrounding atoms. In principle, we have to write down a multielectron Hamiltonian describing the degenerate states of the d shell, and including Coulomb and exchange interactions. However, as we show below it is usually sufficient to consider the non-degenerate version of this Hamiltonian

$$H_d = \sum_{i\sigma} \left(E_d \hat{n}_{i\sigma} + \frac{U}{2} \hat{n}_{i\sigma} \hat{n}_{i-\sigma} \right), \quad (3)$$

which simplifies the calculation considerably. Here E_d is the atomic energy level of the localized Mn t_2 -electrons and U is the Anderson-Hubbard repulsive parameter; $\hat{n}_{i\sigma} = d_{i\sigma}^\dagger d_{i\sigma}$ is the occupation operator for the manganese t_2 - electrons on the impurities, labelled $i = 1, 2$ in (III,Mn)V DMS. The situations when the degeneracy of the t_2 states is important and the exchange interaction (Hund rule) in the multielectron atom starts playing an essential part will be outlined and the appropriate corrections will be introduced, when necessary.

The last term in Eq. (1) describes the scattering of heavy holes by the impurities

$$H_{hd} = H_{hd}^{(r)} + H_{hd}^{(p)}, \quad (4)$$

$$H_{hd}^{(r)} = \sum_{\mathbf{p}, \sigma, j} \left(V_{\mathbf{p}d} c_{\mathbf{p}h\sigma}^\dagger d_{i\sigma} e^{i\mathbf{p}\mathbf{R}_j/\hbar} + h.c. \right),$$

$$H_{hd}^{(p)} = \sum_{\mathbf{p}\mathbf{p}', \sigma, j} W_{\mathbf{p}\mathbf{p}'} c_{\mathbf{p}h\sigma}^\dagger c_{\mathbf{p}'h\sigma} e^{i(\mathbf{p}-\mathbf{p}')\mathbf{R}_j/\hbar}.$$

Here $V_{\mathbf{p}d}$ is the p - d hybridization matrix element, and $W_{\mathbf{p}\mathbf{p}'}$ is the scattering matrix element due to the difference of the pseudopotentials of the host and the substituted atoms. The direct overlaps between the d -electron wave functions of the neighboring impurities in the DMS and the Coulomb interaction between them are neglected.

As mentioned above, the orbital degeneracy of the t_2 states is not taken into account in this simplified model. In reality, the orbital quantum numbers are important at least

in three respects. First, the half-filled d^5 subshell of Mn is occupied by e and t_2 electrons with parallel spins in accordance with the Hund rule, so the sixth electron can be captured in the d^6 configuration only with the opposite spin. The energy cost of this capture is $\sim U + J$, where $J \ll U$ is the exchange energy. This feature of the impurity is preserved in the above simplified Hamiltonian: (3) the reaction $d^5 + e \rightarrow d^6$ is changed for $d^1 + e \rightarrow d^2$, with the spin of the second electron opposite to the first one. The energy cost of this reaction is U , and the principal features of the ion, important for the formation of the localized magnetic moment, are practically the same as in the original atom.

Second, it is the Hund rule that requires that the total angular moments of the Mn atoms be parallel to allow the indirect inter-impurity interaction between the high-spin d^5 states via the hh valence band states. We will take the Hund rule explicitly into account, when calculating T_C , and it will be shown below, that the energy gain due to this indirect interaction, monitored by the Hund rule, leads eventually to ferromagnetic ordering in DMS's.

Third, the three-fold degeneracy of the t_2 electrons is also manifested in the statistics of the localized states, and therefore it influences the position of the Fermi energy in the energy gap. These statistics are described in the Appendix. The degeneracy introduces also numerical factors in the effective exchange constants. These factors are also calculated in the Appendix.

Having all this in mind, we proceed with the derivation of the indirect inter-impurity exchange within the framework of the non-degenerate Alexander-Anderson model, whereas the corresponding corrections for the real orbital structure of the Mn ion will be made when necessary. To calculate the energy of the exchange interaction between two magnetic impurities, one should find the electronic spectrum of the semiconductor in the presence of two impurities. Each impurity perturbs the host electron spectrum within a radius r_b . Inter-impurity interaction arises, provided the distance between the impurities R_{ij} is comparable with $2r_b$. General equations for the two-impurity states and the corresponding contribution to the exchange energy are derived in Appendix. Here we present only the final equations, which will be used in the derivation of the effective exchange coupling and the Curie temperatures for the specific DMS's.

The quantity, which we actually need here is the impurity related correction to the energy of the system. It is given by the standard formula (see, *e.g.*, Ref. 32,50)

$$E^{magn} = \frac{1}{\pi} \text{Im} \int_{-\infty}^{\infty} \varepsilon \cdot \text{Tr} \Delta G[\varepsilon - i\delta \text{sign}(\varepsilon - \mu)] d\varepsilon - \sum_i U n_{di\uparrow} n_{di\downarrow}. \quad (5)$$

$\Delta G = G(\varepsilon) - \mathbf{g}^0(\varepsilon)$ is the two impurity correction to the total one-particle Green function $G(\varepsilon) = (\varepsilon - \mathbf{H})^{-1}$

Here \mathbf{G} is defined as a matrix in (h, d) space, and \mathbf{g}^0 is the same matrix in the absence of impurity scattering, see Eq. (A8). The Green function is calculated in the self-consistent Hartree-Fock approximation for the inter-impurity electron-electron repulsion U , which is sufficient for a description of magnetic correlations in TM impurities in semiconductors. This solution is described in the Appendix. Then the part of the two-impurity energy (5) responsible for the inter-impurity magnetic interaction may be found (see Eqs. (A17) and (A18)). As shown in Refs. 31,45, the resonance scattering alone may result in creation of

CFR and DBH levels split off from the valence band, provided the scattering potential is comparable with the bandwidth. However, in the case of shallow DBH states the potential scattering may dominate their formation. Like in the well-known Koster-Slater impurity model, the potential scattering in our model is described by a short-range momentum independent coupling constant, $W_{\mathbf{pp}'} \approx W$, and the same approximation is adopted for the resonance scattering parameter, $V_{\mathbf{pd}} \approx V$.

Then (5) acquires the compact form

$$\Delta E = -\frac{1}{\pi} \text{Im} \int_{\varepsilon_{hb}}^{\varepsilon_F} d\varepsilon [\ln R^\sigma(\varepsilon) + \ln Q^\sigma(\varepsilon)] + E_{loc}(\varepsilon < \mu). \quad (6)$$

Here the first term in the r.h.s. describes the band contribution to the exchange energy, and the integration is carried out from the bottom of the hh band (ε_{hb}) to the Fermi level ε_F . In this integral the kinetic energy gain of the band electrons due to scattering by ferromagnetically aligned impurities is incorporated. The contributions of resonance and potential scatterings are given by the first and second term in this integral, respectively. The last term ΔE_{loc} is the contribution of the occupied localized CFR and/or DBH states. These states are described by zeros of the functions $R^\sigma(\varepsilon)$ and $Q^\sigma(\varepsilon)$ in the discrete part of the energy spectrum (see Eqs. (A11) and (A9), respectively).

In all the cases the energy gain results from the indirect spin-dependent inter-impurity overlap, and the mechanism of the effective exchange interaction may be qualified as kinematic exchange. In general, double exchange favors a FM order, because the splitting of the energy levels belonging to two adjacent impurities occurs due to electron hopping via unoccupied band or impurity-related states *without spin reversal*. Were the impurity angular moments non-parallel, the Hund rule would suppress the probability of the electron, with spin parallel to the first impurity angular momentum, to hop onto the second impurity with a "wrong" direction of the angular momentum.

The level splitting, when not suppressed by the Hund rule, results in an energy decrease provided that not all of the available band and impurity levels are occupied. One should note that this kinematic exchange cannot be reduced to any conventional double exchange mechanism because of an actual interplay between three contributions to the magnetic energy, namely, the scattered valence band electrons, the CFR states and the DBH states. We start with the analysis of the band contribution $\Delta E_{b,ex}$. Since in all the cases we deal with nearly filled hh bands, it is convenient to calculate the energy in the hole representation.

By means of a simple trick (as described in the Appendix) the contribution of the hh band in the basic equation (6) may be transformed into

$$\Delta E_{b,ex} = \frac{1}{\pi} \text{Im} \int_{\varepsilon_F}^{\varepsilon_{ht}} d\varepsilon \ln \frac{R^\sigma(\varepsilon)}{R_0^\sigma(\varepsilon)}, \quad (7)$$

where ε_{ht} stands for the top of the valence band. This equation is obtained from the more general equation (A21) by neglecting the potential scattering in the band continuum. Then, inserting Eq. (A11) for the matrix $R^\sigma(\varepsilon)$ we obtain

$$\Delta E_{b,ex} = -\frac{1}{2\pi} \text{Im} \int_{\varepsilon_F}^{\varepsilon_{ht}} d\varepsilon \ln \left\{ \frac{[g_d^{-1}(\varepsilon - i\delta) - V^2 L_{11}(\varepsilon - i\delta)]^2 - V^4 L_{12}^2(\varepsilon - i\delta)}{g_d^{-1}(\varepsilon - i\delta) - V^2 L_{11}(\varepsilon - i\delta)} \right\}. \quad (8)$$

Here

$$L_{ij}(\varepsilon - i\delta) \equiv P_{ij}(\varepsilon) + \frac{i}{2}\Gamma_{ij}(\varepsilon) \quad (9)$$

are the standard lattice Green functions (A10) of the continuous argument ε . Retaining only the leading (quadratic) terms in L_{12} in Eq. (8), the exchange energy due to the hh band becomes

$$\Delta E_{b,ex} = -\frac{V^4}{\pi} \int_{\varepsilon_F}^{\varepsilon_{ht}} d\varepsilon \frac{P_{12}(\varepsilon)\Gamma_{12}(\varepsilon)}{[\varepsilon - E_d - V^2 P_{11}(\varepsilon)]^2 + \frac{V^4}{4}\Gamma_{11}^2(\varepsilon)}. \quad (10)$$

Eq. (8) with $L_{12}(\varepsilon) \neq 0$ holds only if the impurity angular moments are parallel to each other (ferromagnetic case), since the electron hopping between the impurities via the hh band takes place without spin-flips. If the angular moments are non-parallel, the Hund energy does not allow the electron to hop to the neighboring impurity with a "wrong" angular momentum direction. So the impurities with non-parallel angular moments cannot exchange their electrons, which effectively means that for them $L_{12} = L_{21} = 0$. Thus, Eq. (10) is the energy decrease due to the kinematic indirect exchange between a pair of magnetic impurities with parallel angular moments. If the moments are not parallel the corresponding energy decrease is zero.

Another contribution to the magnetic energy ΔE (Eq. (6)) originates from the inter-impurity hopping via empty localized states, if available. As was mentioned above, there are two types of such states, namely CFR and DBH-type levels. For the CFR states, one may, to a good approximation, neglect the potential impurity scattering. To take properly into account the Coulomb blockade effect on the impurity site, one has to calculate the Green function in a self-consistent way, known as "Hubbard I" approximation (see Eqs. (A11), (A16) in the Appendix).

As was pointed out above, the origin of the energy gain is the inter-impurity level splitting. The latter is derived in the Appendix (Eqs. (A22) and (A23)). The result is

$$\delta E_{CFR\pm} = \pm\Delta + \frac{9K^2}{2} \frac{V^4}{[1 - KV^2 P'_{11}]^2} \frac{dP_{12}^2}{d\varepsilon}, \quad (11)$$

where the splitting of the levels of the isolated impurities is

$$\Delta(\mathbf{R}) = \frac{KV^2 P_{12}(\mathbf{R})}{1 - KV^2 P'_{11}}. \quad (12)$$

The second term in Eq. (11) results from the repulsion of the two-impurity levels from the band continuum. All the functions P_{ij} and their derivatives P'_{ij} are taken at $\varepsilon = E_{CFR}^0$, i.e. at their positions for the isolated impurities (A22).

Considering the contribution of the DBH states we may apply the procedure outlined in the Appendix and to find the kinematic exchange due to the DBH states lying above the top of the valence band

$$\Delta E_{DBH,ex} = \frac{KV^2 P_{12}^2}{(E_{DBH}^0 - E_d - V^2 P_{11})P'_{11}}. \quad (13)$$

Now all the functions in Eq. (13) should be calculated at the DBH level ($\varepsilon = E_{DBH}^0$). This part of the kinematic exchange favors the ferromagnetic ordering, since $P'_{11}(E_{DBH}^0) < 0$. If the DBH levels lie not too far from the top of the valence band their contribution may be comparable with that of the hole pockets and should be properly taken into account when calculating the Curie temperature. At a sufficiently high Mn content the splitting of the DBH level may result in the formation of an impurity band and its merging with the hh band. This case is discussed in the next section.

Thus one sees that the contribution, ΔE_{loc} , of the localized states to the kinematic exchange *is not universal*. It depends on the type of conductivity and should be considered separately for p - and n -type materials. In the p -type samples one should take into account the empty shallow Mn-related levels, which are present in p -(Ga,Mn)As and p -(Ga,Mn)P and apparently absent in p -(Ga,Mn)N. In the n -type (Ga,Mn)N, the localized states are due to the deep Mn CFR levels, and hopping over these levels alone determines the exchange mechanism. The double exchange mechanisms in these two cases are obviously different.

To calculate the Curie temperature T_C for the p - and n -type materials one should extend the two-impurity calculations for dilute materials with small Mn concentration x and take into account the corresponding transformations in the magnetic energy. This program is realized in the two next sections.

III. MAGNETIC ORDER IN P -TYPE DMS

Here we discuss the formation of ferromagnetic order in Mn-doped III-V p -type semiconductors. (Ga,Mn)As together with (Ga,Mn)P are the most celebrated among them. As mentioned above, the CFR level of the fifth d electron lies in these systems below the heavy hole band. A DBH level is also formed above the top of the valence band. At sufficiently high concentrations these DBH levels start broadening into an impurity band, and may merge with the valence band. The band structure of (Ga,Mn)As is shown schematically in Fig. 1.

The empty localized levels lying above the Fermi energy. (While making fitting of the theory to experimental data we use the Fermi energy ε_F instead of the chemical potential μ , since they nearly coincide under the condition of the experiment.) appear due to the combined action of both the potential (W) and resonance (V) scattering mechanisms. Formally they can be found as zeros of the determinant $R(\varepsilon)$ (see Eq. (A11)). Neglecting small corrections due to resonance scattering, the energy of an isolated DBH level, $E_{DBH}^0 \equiv \varepsilon_i$, corresponds to a zero of the function

$$q(\varepsilon_i) = 1 - WP_{11}(\varepsilon_i) = 0, \quad (14)$$

like in the Koster-Slater one-impurity problem (see the graphic solution on the left panel of Fig. 1). The calculations below will be carried out assuming the model semi-elliptic density of states for the hh band

$$\rho(\varepsilon) = \frac{2}{\pi w^2} \sqrt{w^2 - 4 \left(\varepsilon - \frac{w}{2} \right)^2},$$

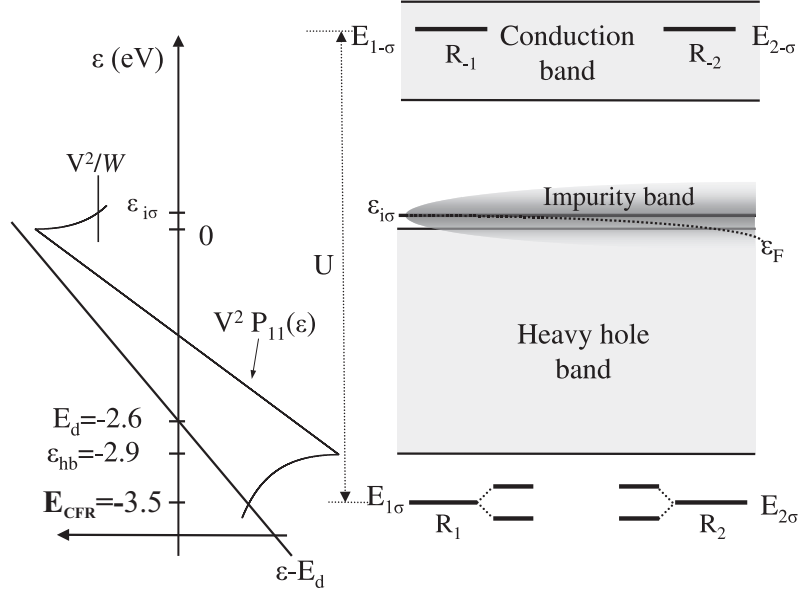


FIG. 1: Left panel: graphical solution of Eq. (17) for the bonding CFR and Eq. (14) for the antibonding DBH levels. Right panel: energy levels in (Ga,Mn)As. The CFR d-levels d^5/d^4 (denoted by $R_{1(2)}$) of each impurity, lie below the hh band. The DBH levels (energies $\varepsilon_{1\sigma}$, $\varepsilon_{2\sigma}$) are split from the hh band and form localized (acceptor) levels in the energy gap. The CFR levels d^6/d^5 $R_{-1(-2)}$ lie high in the conduction band. The impurity band is shown by the shaded area together with the position of the Fermi level as a function of the width of the impurity band (horizontal axis)

where w is the hh bandwidth and the energy ε is counted from the top of the hh band. Then the position of the acceptor DBH level can be found explicitly

$$\varepsilon_i = E_{DBH}^0 = W \left(1 - \frac{w}{4W}\right)^2.$$

Using a realistic value $w = 2.9eV^{52}$ for the hh bandwidth and taking the matrix element of the potential scattering $W = 1.02$ eV, one obtains the acceptor level position $\varepsilon_i = 85meV$ for (Ga,Mn)As. The influence of resonance scattering on the positions of the shallow DBH levels of the two interacting impurities may be usually neglected (see Ref. 45 for a detailed description of the interplay between resonance and potential impurity scattering).

At a sufficiently high impurity content, x , an impurity band is formed in (Ga,Mn)As since the DBH levels are split due to the indirect interaction within the impurity pairs. We neglect the pd -hybridization V , keep only the contribution of the potential scattering (W) and obtain

$$\delta\varepsilon_{\pm} = -\frac{1}{WP_{11}'}\mathbf{q}_{\pm}, \quad (15)$$

where \mathbf{q}_{\pm} are the two solutions of Eq. (A25).

Then Eqs. (15) and (A25) result in

$$\Delta_{DBH}(\mathbf{R}) \equiv \frac{1}{2}(\delta\varepsilon_+ - \delta\varepsilon_-) = -\frac{P_{12}(\mathbf{R})}{P_{11}'}$$

The functions P and P' are calculated at $\varepsilon = \varepsilon_i$. The half-width of the impurity band can be roughly estimated as $z\Delta_{DBH}(\bar{R})$ where \bar{R} is the typical distance between the impurities, which depends on the impurity content x . The z value characterizes the number of neighboring impurities participating in the interaction with any given impurity. If the half-width $z\Delta_{DBH}(x)$ of the impurity band exceeds the energy ε_i (counted from the top of the valence band), the impurity band merges with the valence band and they both form a unified continuum of states. For the above mentioned values of the model parameters this merging occurs even at $x < 0.01$.

Eventually, the magnetic order is due to the exchange interaction between the occupied CFR levels. These levels correspond to the states d^5/d^4 of the Mn ions below the hh band, whereas the empty d^6/d^5 CFR levels are pushed up to the conduction band by the Anderson-Hubbard repulsion U (Fig. 1).

The left panel of this figure depicts a graphical solution of the equation

$$R(\varepsilon) = 0, \quad (16)$$

with $R(\varepsilon)$ defined in Eq. (A11). Neglecting the interaction between the impurities, $L_{12} = 0$ (and, hence $M_{12}(R) = 0$), Eq. (16) takes the form

$$E_{CFR} \equiv E_{i\sigma} = E_d + V^2 L_{ii}(E_{i\sigma}), \quad (17)$$

and describes the formation of the deep impurity states of CFR type out of the atomic d -levels E_d below the hh valence band. The values of the parameters used in the graphical solution presented in Fig. 1 will be discussed below.

For a finite distance between the impurities, the overlap of impurity wave functions due to the nonzero $L_{12}(R)$ leads to a level splitting as shown in the right panel of Fig. 1. Each of the two impurity levels is singly occupied due to the Anderson-Hubbard on-site repulsion. The inter-impurity overlap arises due to the pd -hybridization, which does not involve spin-flips, hence it occurs only for the parallel impurity angular moments (Hund rule). There is no level splitting for the non-parallel impurity angular moments, unless one takes into account indirect interaction via empty d^6 states.

FM ordering arises, provided the state with the parallel impurity angular moments is energetically preferable in comparison to that with the non-parallel ones. It is obvious that the splitting per se cannot give an energy gain, when both states are occupied. One should take into account all the changes in the energy spectrum, namely, the reconstruction of the *partially filled* merged impurity and hh band. The indirect interaction involving empty states near the top of the hh band is in fact *a novel type of the double FM exchange*, which resembles the well known Zener exchange³⁶ but differs from it in many important aspects (see below).

The contribution favoring the FM order can be obtained from Eq. (10) with the addition of the part due to the impurity band merged with the valence band,

$$\Delta E_{FM} = -\frac{V^4}{\pi} \int_{\varepsilon_F(x)}^{\varepsilon_i + z\Delta_{DBH}(x)} d\varepsilon \frac{\Gamma_{12}(\varepsilon)P_{12}(\varepsilon)}{[\varepsilon - E_d - V^2 P_{11}(\varepsilon)]^2 + \frac{V^4}{4}\Gamma_{11}^2(\varepsilon)}, \quad (18)$$

(the reference energy in this equation is taken at the top of the hh band). In the FM-aligned spin configuration only the *majority* spin subband contributes to ΔE_{FM} , therefore the spin index is omitted for the sake of brevity.

We use in our numerical estimates the following approximate relations,

$$\begin{aligned} P_{11}(\varepsilon) &= P_{22}(\varepsilon) = \int d\omega \frac{\rho(\omega)}{\varepsilon - \omega}, & P_{12}(\varepsilon) &= \int d\omega \frac{\sin[k(\omega)R]}{k(\omega)R} \frac{\rho(\omega)}{\varepsilon - \omega}, \\ \Gamma_{12}(\varepsilon) &\approx 2\pi\rho(\varepsilon) \sin[k(\varepsilon)R]/k(\varepsilon)R, & \Gamma_{11}(\varepsilon) &\approx \pi\rho(\varepsilon) = \Gamma_{22}(\varepsilon). \end{aligned} \quad (19)$$

(here R is the inter-impurity distance). The value of the wave-vector k is found from the equation $\varepsilon = \varepsilon_{hh}(k)$, where $\varepsilon_{hh}(k)$ is the hh energy dispersion. In our model calculations the impurity band merges with the top of the valence band of (Ga,Mn)As at the concentration $x_{crit} = 0.0065$ with the renormalized 3d-wave-function enveloping 5 to 6 unit cells. Earlier transport measurements for low T_C samples indicate merging even at $x = 0.002$. All this justifies the approximation adopted for the hole state in Eq. (18). This equation is our working formula, from which we obtain T_C .

The mechanism outlined above competes with the antiferromagnetic (AFM) Anderson-type superexchange⁴⁹ involving the empty d^6 states. The energy gain in the latter case is estimated as

$$\Delta E_{AFM} \approx -V^4 L_{12}^2 / U. \quad (20)$$

It should be compared with the above Zener-type mechanisms. We assume that

$$P_{ij} \sim w^{-1}, \quad \Gamma_{ij} \sim \varepsilon_F^{1/2} w^{-3/2}, \quad \varepsilon_F - E_d - V^2 P_{11}(\varepsilon_F) = 4\alpha V^2 / w,$$

with $\alpha < 1$ (see left panel of Fig. 1). Then one finds from Eqs. (18) and (20) that $|\Delta E_{AFM}| \sim V^4 a^2 \exp(-2\kappa_b R_{12}) / (U w^2 R_{12}^2)$, with $\kappa_b = \sqrt{2m(\varepsilon_{bh} - E_{d\sigma})} / \hbar$, $|\Delta E_{FM}| \sim 2\varepsilon_F (\varepsilon_F / w)^{1/2} / [(4\alpha)^2 + \varepsilon_F / (4w)]$ and FM coupling is realized provided $|\Delta E_{FM}| > |\Delta E_{AFM}|$, which normally takes place since the parameter U is large. Numerical estimates are given below.

Now the difference between the double exchange mechanism in DMS and the Zener double exchange in transition metal oxides becomes clear. The conventional Zener double exchange mechanism was proposed³⁶ for (La, A²⁺)MnO₃. In this case Mn ions are in different valence states (Mn³⁺ and Mn⁴⁺). In our case it would have meant that one of the two levels $E_{CFR\uparrow}$ were empty. It is seen from Fig. 1 that in (Ga,Mn)As both these states are occupied, and the Zener mechanism in its original form is not applicable. Actually, the FM order in the p -type DMS arises due to the kinematic exchange between the two Mn(d^5) ions via the empty states near the top of the valence band.

In order to calculate the exchange energy Eq. (18), the dependence of the Fermi level on the Mn content $\varepsilon_F(x)$ should be known. It is found from the equation

$$x_s = 2 \int_{\varepsilon_F(x)}^{\delta w(x)} \rho(\varepsilon) d\varepsilon, \quad (21)$$

$\delta w(x) = \varepsilon_i + z\Delta_{DBH}(x)$, and the hh density of states is approximated as

$$\rho(\varepsilon) = 8 / [\pi (w + \delta w(x))^2] \sqrt{[\delta w(x) - \varepsilon] (\varepsilon + w) \theta[\delta w(x) - \varepsilon] \theta(\varepsilon + w)}.$$

(z is the coordination number in the impurity band). The per site hole concentration x_s is proportional to the hole density p_h ; $x_s = a^3 p_h / 8$ in the zinc-blende structure. Equations (18) and (21) allow one to determine the pair exchange energy as a function of Mn concentration x and connect it with the experimental data for the given hole concentrations $p_h(x)$ which are taken from the measurements.⁵³

The Curie temperature T_C was calculated in the molecular field approximation. According to this approach the spin Hamiltonian reads

$$H_{MF} = \frac{1}{2} \sum_i \Delta E_{FM}(\mathbf{R}_{ij}) \mathbf{J}_i \cdot \langle \mathbf{J} \rangle, \quad (22)$$

where summation runs over all positions of the Mn impurities with an angular momentum operator \mathbf{J}_i . Here the factor 1/2 accounts for the fact that the energy gain of the FM vs AFM orientation of two coupled spins is $\Delta E_{FM}(\mathbf{R}_{ij})$, contrary to $2J_{Heis}$ in the Heisenberg model. Then the Curie temperature can be readily found,

$$T_C = -\frac{\Delta E_{FM}(x) \bar{z} J(J+1)}{k_B 6}. \quad (23)$$

where \bar{z} is, similarly to z , a measure of the neighboring atoms participating in the exchange interaction. It is certainly close to z , although it does not necessarily coincide with it. It is worth mentioning here that unlike the case of magnetically doped metals⁵⁰ we cannot represent the effective inter-impurity coupling in the asymptotic form

$$\Delta E_{FM}(R_{ij}) \sim \cos(2k_F R_{ij} + \phi) / (k_F R_{ij})^3$$

because typically $k_F^{-1} \sim F R_{ij}$ in doped semiconductors.

In (Ga,Mn)As the total angular momentum of a complex $\text{Mn}(3d^5\bar{p})$ is unity³⁸: $J = 1$, since it is formed by the moment $j = 3/2$ of the loosely bound hole AFM-coupled to the Mn center with the spin $S = 5/2$. Then the numerical factor in Eq. (23) is close to unity. The results of our calculations are presented at Figs. 2 and 3.

In order to find the dependence $T_C(x)$, the calculated value of the Fermi level via Eq. (21), based on the experimental data of Ref. 53, is used in Eqs. (23) and (18). A polynomial fit is used for the hole density $p_h(x)$ in Eq. (18). The values of the model parameters characterizing the impurity d -state are $U \approx 4.5$ eV, $V = 1.22$ eV, while the hh mass $m = 0.51 \cdot m_0$ and hh bandwidth $w = 2.9$ eV were taken from Ref. 52. The hybridization strength V was obtained from Eq. (17) with $E_{CFR} = -3.47$ eV ($E_{CFR}^{\text{exp}} = -3.4$ eV according to Ref. 56). The value of $\varepsilon_i = 85$ meV was chosen for the energy of the shallow acceptor level (not far from the experimental value³⁴ $\varepsilon_i^{\text{exp}} = 110$ meV.) The value of $\bar{z} = 2.5$ was taken for the coordination number in as-grown samples (Fig.2, lower curve). At these values for the model parameters the ratio $|\Delta E_{FM}|/|\Delta E_{AFM}| \sim 2$ justifies the dominance of the FM coupling in (Ga,Mn)As.

The non-monotonous dependence $T_C(x)$ is due to a non-equilibrium character of the sample preparation. Apparently, the ratio between the concentration of Mn impurities and the actual hole concentration depends on the doping method and the thermal treatment. In particular, the annealing of the sample results in a reduction of the donor-like Mn-related interstitial defects in favor of acceptor-like substitution impurities.^{53,58} To describe

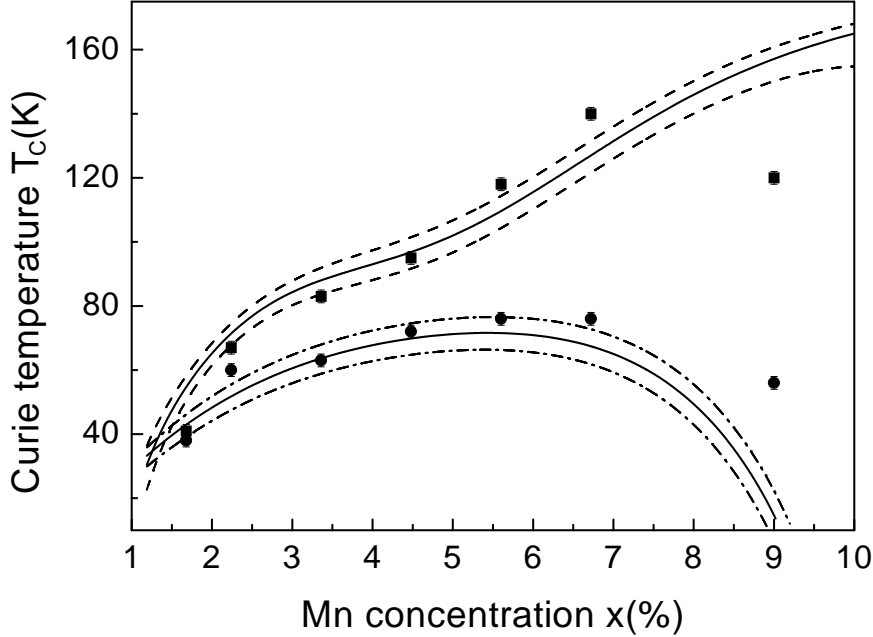


FIG. 2: Calculated dependence of T_C on the manganese concentration x in (Ga,Mn)As based on the experimental data for the hole density⁵³ $p_h(x)$. Solid squares (circles) stand for experimental $T_C(x)$ of annealed (as-grown) samples. Broken lines take into account the error bars of the hole density.

the annealing effect we changed the value of \bar{z} from 2.5 to 4 in Eqs. (18) and (23). The results of numerical fitting are shown in the upper curve of Fig. 2.

Recent detailed measurements of the hole concentrations in a series of both as-grown and annealed $\text{Ga}_{1-x}\text{Mn}_x\text{As}$ samples,⁵³ allowed us to compare the theoretical plot $T_C(p)$ with the experimental data. These results are presented in Fig. 3. Our fitting procedure uses the same equations (23) and (18), and the same values for the model parameters E_{CFR} , U , ε_i as in the above estimate. The Mn concentration point $x = 0.067$ is used as a reference point, and the coordination number $\bar{z} = 4$ is chosen. Two theoretical curves correspond to two values of the hybridization parameter $V = 1.22$ and 1.24 eV (solid and dash-dotted curves, respectively). One may conclude from these two fittings that the theory is not very sensitive to the choice of the model parameters. To check this statement, we made one more fitting of the experimental data obtained only for annealed samples. (see Fig. 4). These data are taken from Ref. 58. We see that the calculations with the same set of model parameters give satisfactory quantitative agreement with the experiment for these samples as well.

Thus, our theory provides a satisfactory quantitative description of the behavior of the Curie temperature T_C as a function of the Mn content x and the hole concentration p_h in p -(Ga,Mn)As. This description is applicable also to p -(Ga,Mn)P. The band structure

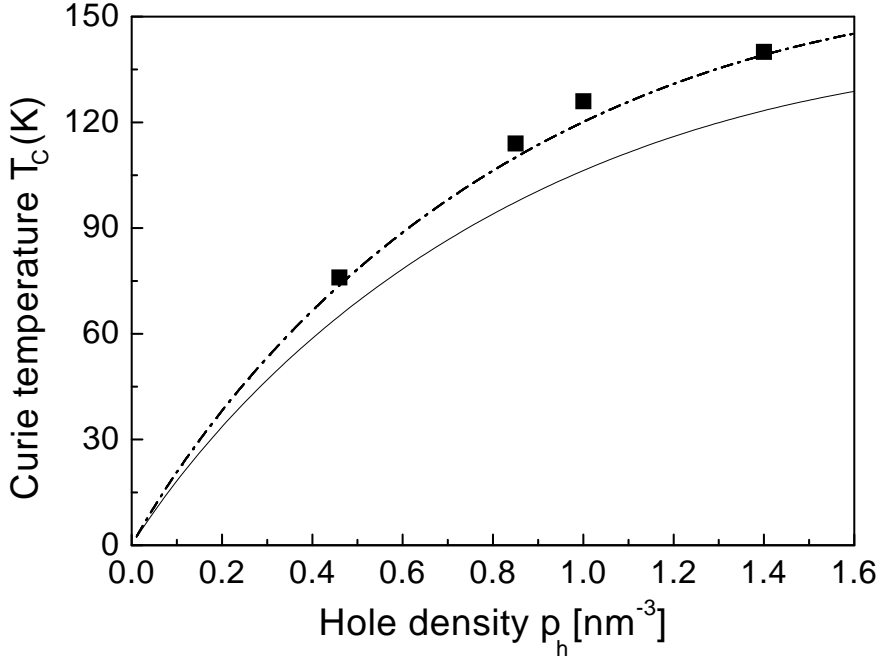


FIG. 3: The dependence of the Curie temperature on the hole density p in (Ga,Mn)As. Solid and dash-dotted lines are the theoretical curves for the two values of the hybridization parameter ($V = 1.22$ and 1.24 eV, respectively). Experimental points (filled squares) are taken from Ref. 53.

of (Ga,Mn)P can be also schematically represented by Fig.1, however, the DBH level lies deeper in the energy gap than in p -(Ga,Mn)As: its position is estimated as ≈ 0.4 eV above the top of the valence band (see, e.g. Refs. 33,34,47,52). The impurity band appears to be narrower than in (Ga,Mn)As. It does not merge with the hh band at any reasonable Mn concentration and its contribution to the indirect exchange can be neglected. We tested our theory by fitting the experimental value⁵⁴ of $T_C = 270$ K reported for a p -type (Ga,Mn)P at $x = 0.06$. The impurity level $\varepsilon_i = 400$ meV arises at $W = 1.4$ eV. We have found that the value of $T_C = 270$ K is reproduced by means of Eq. (23) with the following fitting parameters: $w = 2.6$ eV, $V = 1.31$ eV, $x = 0.05$, $\bar{z} = 4$, $E_d = -1.3$ eV (then $E_{CFR} = -3.28$ eV). The chosen value of $p_h = 1 \cdot 10^{20} \text{ cm}^{-3}$ is the hole density in a C-doped GaP before Mn implantation.⁵⁴ So the values of our model parameters are close to those for (Ga,Mn)P in the experiments of Ref. 54. Besides, these parameters are in a good correlation with the chemical trends in the systems (Ga,Mn)As, (Ga,Mn)P (the latter has a smaller lattice spacing and larger effective mass m_{hh}^* than the former).

As for p -(Ga,Mn)N, the theory should be somewhat modified in order to describe this material. In this case Mn remains a neutral substitution isoelectronic defect in the configuration $\text{Mn}^{3+}(d^4)$, since the $\text{Mn}^{2+/3+}$ transition energy falls deep into the wide energy gap in accordance with the experimental⁴⁷ and theoretical³⁰ data. If the hole

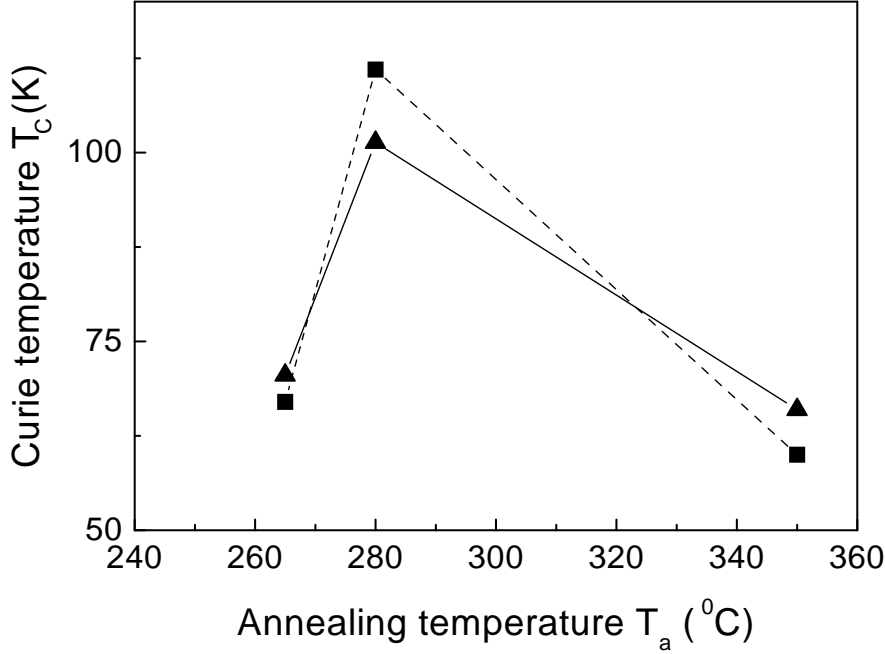


FIG. 4: Calculated T_C (triangles connected by a solid line) vs the annealing temperature T_a in (Ga,Mn)As. The data for the hole density and the experimental values of $T_C(T_a)$ (closed squares) are taken from Ref. 58. The parameters used in the calculations are: $V = 1.22eV$, $\bar{z} = 4.0$, $E_{CFR} = -2.6eV$.

concentration, p_h , exceeds the Mn content, x , then we return to the situation discussed in this section, but with the localized moment $J = 2$ characteristic of the $Mn^{3+}(e^2t^2)$ configuration. In the opposite case, the valence band is full, and the Fermi energy lies within the deep impurity band formed by the $Mn^{2+/3+}$ levels. This situation is discussed in the next section.

Unfortunately, there are not enough experimental data on $T_C(x)$ available to make a detailed comparison with the theoretical predictions both in p -(Ga,Mn)P and p -(Ga,Mn)N materials. Moreover, no p -type conductivity was observed in (Ga,Mn)N even in the cases when the pristine GaN crystals were of a p -type. Due to the lack of experimental information, we have confined ourselves with a quantitative description of the p -type (Ga,Mn)As and turn now to the case of n -(Ga,Mn)N, where the double exchange mechanism, as described above, should be revisited.

IV. MAGNETIC ORDER IN N-TYPE DMS

In accordance with the general predictions of the theory,^{33,34} Mn is a deep acceptor in GaN, and each Mn impurity creates an *empty* t_2 level close to the middle of the energy

gap of GaN. Therefore, the Fermi energy should be pinned to these levels unless other (shallow) acceptors create enough free holes near the top of the valence band. This statement is confirmed by extended cluster "quasi band" calculations.³⁰ If a Mn-doped sample contains also shallow donors in a noticeable concentration, then the deep Mn-related impurity band is partially filled by electrons, and one arrives at the problem of magnetic order in n -type (Ga,Mn)N.

In this case the d^5/d^4 CFR energy levels forming the impurity band are partially filled, so one encounters the mixed valence $\text{Mn}^{3+}/\text{Mn}^{2+}$ situation similarly to the original Zener model.³⁶ Hopping in the impurity band is possible due to an overlap of the tails of the impurity wave functions. These tails are formed by the superpositions of the Bloch electron wave functions from the hh band, so the latter in fact plays the role which is similar to that of the oxygen p-orbitals in $\text{La}(\text{Mn,Sr})\text{O}_3$ considered by Zener.

The specific feature of the n -type (Ga,Mn)N DMS's is that the d^5/d^4 CFR impurity levels, E_{CFR} , lie deep within the forbidden energy gap. At a high enough Mn content they may form an impurity band, which still remains well separated from the hh band. This impurity band may be partially occupied by electrons and be responsible for the possible magnetization of the DMS. To describe formation of a deep impurity band within the framework of our model, we solve Eq. (17) for a Mn-related CFR level and then substitute this solution into the secular equation (16). These calculations are performed by using the same semi-elliptic density of valence states $\rho(\varepsilon)$ as in Section III. The bare level E_d in this case is above the top of the hh band, and the pd hybridization only slightly renormalizes its position in the energy gap. The graphical solution of Eq. (17) is presented in the left panel of Fig. 5.

We assumed that the hybridization parameter is nearly the same as in (Ga,Mn)As, $V = 1.2$ eV. The right panel of Fig. 5 illustrates the formation of an impurity dimer via an overlap of the tails of the CFR wave functions in accordance with Eq. (16). Then the electron hopping between the correlated states R_1 and R_2 initiates formation of an impurity band and the Zener type indirect exchange interaction arises, provided the impurity band is partially occupied. In principle, the double exchange via empty states in conduction band should be taken into account. However, this contribution is small in zinc blende host crystals, because the hybridization V_{ds} between the impurity d -states and the s -states of the electrons near the bottom of conduction band is weak due to the symmetry selection rules.^{33,34} The empty (d^6/d^5) CFR levels are pushed up high to the conduction band by the Anderson-Hubbard repulsion U . Like in the previous case these levels can be a source of AFM ordering in the impurity band, but we do not consider this relatively weak mechanism here. Another contribution to indirect exchange in the case of n -(Ga,Mn)N is the fourth-order in $|V_{dp}|^2|V_{ds}|^2$ Bloembergen-Rowland indirect exchange.⁵⁵ However, this term involves the hybridization with both valence and conduction electron states, so it is small due to the above symmetry ban.

In order to calculate the double exchange interaction in such an impurity band, we consider first a pair of impurities at a distance R from each other. To be definite we assume that the chemical potential μ lies below the level E_{CFR} of an isolated impurity. According to Eq. (12) the interaction between the impurities results in splitting of the impurity levels with half-width $\Delta(R)$, where we neglect its possible dependence on the

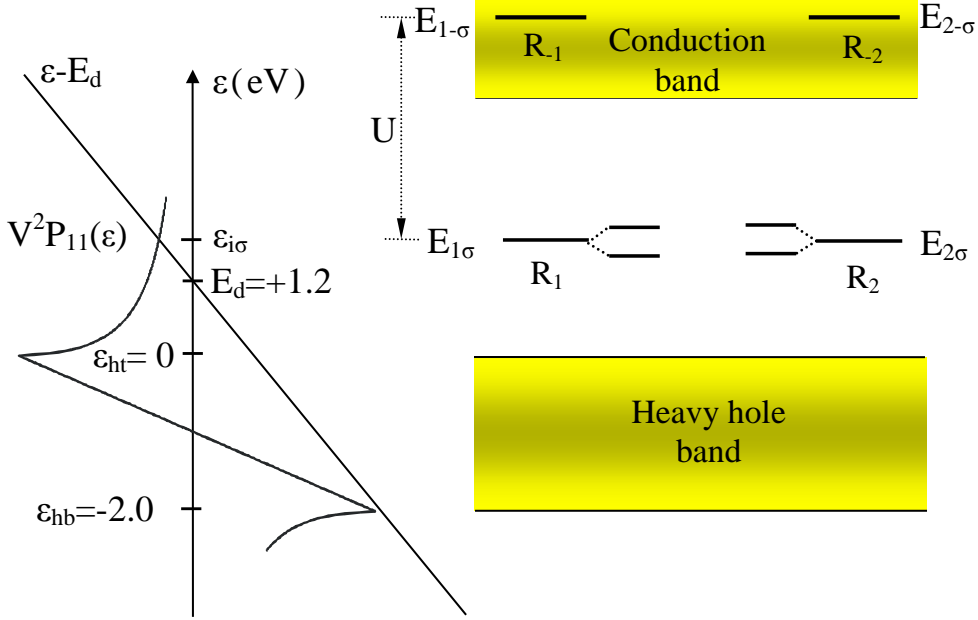


FIG. 5: Left panel: graphical solution of Eq. (17) for the antibonding CFR level in (Ga,Mn)N. Right panel: energy levels in Ga(Mn)N. The CFR d-levels d^5/d^4 (denoted by $R_{1(2)}$) of each impurity, lie within the energy gap. The CFR levels d^6/d^5 $R_{-1(-2)}$ lie high in the conduction band.

direction of the vector \mathbf{R} .

It is emphasized here again that the pd hybridization does not involve spin flips. It means that the electron spin does not change its projection in the course of the whole process leading to the indirect exchange, during which the electron is transferred from one impurity to the other and back via band states. This process is possible only if the spins \mathbf{S}_i of the two impurities are parallel. Otherwise the Hund rule will require an additional energy when the electron tries to hop onto the impurity atom with a "wrong" spin orientation.

One may conclude that the indirect exchange interaction within a pair of impurities appears if their angular moments are parallel (FM ordering), and if the distance between the impurities is not too large, i.e.

$$R < R_{ex}(\mu)$$

where $R_{ex}(\mu)$ is the solution of the equation

$$\Delta(R_{ex}) = E_{CFR}^0 - \mu. \quad (24)$$

Then one of the two impurity levels sinks below the chemical potential μ and is occupied by an electron resulting in the energy decrease $\Delta(R)$, whereas the second level remains empty and does not contribute to the energy balance. If the angular moments of the impurities are not parallel, Hund rule forbids the indirect exchange and there is no energy decrease. Therefore, we conclude that the exchange energy in such a pair equals just $-\Delta(R)$. It is zero if at least one of the above two conditions is not met.

The pair exchange interaction can be estimated as

$$\overline{\Delta} = \int_0^{R_{ex}(\mu)} \Delta(R)g(R)dR \quad (25)$$

where $g(R)$ is the impurity pair distribution function. For example, we may assume that the random distribution of the impurities obeys the Poisson law

$$g(R) = \frac{3R^2}{\overline{R}^3} \exp \left\{ -\frac{R^3}{\overline{R}^3} \right\} \quad (26)$$

where \overline{R} is the average distance between the impurities. The latter is connected with the impurity content x by $\frac{4\pi}{3}\overline{R}^3x = d_0^3$, where d_0 is the minimal possible distance between two Mn ions. This assumption may not work too well for relatively high impurity content, since it overestimates the contribution of closely lying impurities. In fact the impurities cannot approach each other to distances smaller than the distance between two neighboring Ga atoms, $a\sqrt{2}/2$, a lattice constant. In such a case corrections should be introduced for these small distances.

In order to complete our calculations, we need also an equation connecting the position of the chemical potential with the electron concentration n in the impurity band. This concentration coincides with the concentration of impurities in the d^5 state, hence

$$n = \int^{\mu} \rho(\varepsilon)n_{d^5}(\varepsilon - \mu)d\varepsilon \quad (27)$$

where $\rho(\varepsilon)$ is the density of states in the impurity band. The distribution $n_{d^5}(\varepsilon - \mu)$ is calculated in the Appendix, Eq. (A16).

Since, in unfilled impurity band the chemical potential and the Fermi level ε_F practically coincide, we use below the latter term as in the case of p -type samples instead of μ . At low temperatures $n_{d^5}(\varepsilon - \varepsilon_F)$ is 1 for $\varepsilon < \varepsilon_F$ and 0 for $\varepsilon > \varepsilon_F$. This allows us to circumvent the calculation of the density of states $\rho(\varepsilon)$ and present the condition (27) in the alternative form

$$n = \int_0^{R_{ex}(\varepsilon_F)} g(R)dR, \quad (28)$$

which is more convenient for our calculations. If an experiment provide us with dependencies of the Curie temperature and the electron concentration on the Mn content, then Eqs. (24) and (28) will allow us to connect the Fermi energy with the electron density in the impurity band and after that to use Eq. (25) in order to calculate the average pair exchange interaction $\overline{\Delta}(x)$ as a function of the impurity content x .

We may now use the theory of dilute ferromagnetic alloys developed in Ref. 60 (see also the review Ref. 61) and arrive at the final result of this procedure, i.e. the Curie

temperature. Unlike the case of (Ga,Mn)As, the magnetic energy in impurity band is determined by the spin S of Mn $3d$ shell, which equals $5/2$ and 2 for d^5 and d^4 configurations, respectively. In our crude approximation it is sufficient only to know that the proportionality coefficient between T_C and $\bar{\Delta}$ is of order of unity:

$$T_C(x) = \frac{S(S+1)}{6k_B} \bar{\Delta}(x) \approx \bar{\Delta}(x)/k_B.$$

At low electron concentrations, when $R_{ex}(\varepsilon_F) > d_0$, only a minor part of the impurities is coupled by the indirect exchange interaction. Using the above averaging procedure for calculating T_C does not hold any more and a percolation type of approach should be applied. The resulting Curie temperature may become low and will decrease exponentially with the concentration.⁶²

The behavior of the Curie temperature for higher electron concentrations, when the Fermi energy lies above the energy E_{CFR}^0 , can be found in a similar fashion. We just have to switch to the hole representation and use the distribution function $3n_{d^4}(\varepsilon - \varepsilon_F)$ instead of $n_{d^5}(\varepsilon - \varepsilon_F)$. (Dealing with holes we have now to account for the three-fold degeneracy of t_2 states.) The function $3n_{d^4}$ is 1 if $\varepsilon > \varepsilon_F$ and 0 if $\varepsilon < \varepsilon_F$. As a result, we will obtain a mirror symmetric dependence of T_C on x in this concentration range.

To get an idea of the behavior of the average kinematic exchange $\bar{\Delta}$ and, hence of the Curie temperature as a function of the Mn content and the position of the Fermi energy, i.e., electron concentration in the impurity band, we can make simple estimates. Consider the case when $\varepsilon_F < E_{CFR}$, then $K = 1$ and according to Eq. (A23) the levels of a pair of impurities separated by the distance R are split by

$$\delta\varepsilon_{\pm} = \pm\Delta(R) = \pm \frac{V^2 P_{12}(R)}{1 - V^2 P'_{11}} \quad (29)$$

where the off-diagonal lattice sum can be estimated as

$$P_{12}(R) = \frac{1}{2\pi} \frac{m d_0^3}{\hbar^2 R} e^{-\kappa R}. \quad (30)$$

Here κ is the localization parameter. (Although we may use the estimate $\kappa \approx \hbar\sqrt{2mE_{CFR}}$, we should not forget that it may be rather crude for really deep levels.) Then

$$\Delta(R) \approx \Delta_0 \frac{d_0}{R} e^{-\kappa R},$$

where the value of Δ_0 depends on the parameters of the system but is generally of the order of 1eV.

The Poisson pair distribution truncated at small distances $R < d_0$ is

$$g(R) = \begin{cases} \frac{3R^2}{R^3} \exp\left\{\frac{d_0^3 - R^3}{R^3}\right\}, & \text{for } R > d_0 \\ 0, & \text{for } R < d_0 \end{cases}. \quad (31)$$

This distribution accounts for the fact that the Mn impurities cannot come closer than at the distance d_0 from each other. For a deep enough level we may assume $\kappa \approx 1/d_0$

and calculate the dependence of the average kinematic exchange $\overline{\Delta}$ on the Mn content and position of the Fermi energy with respect to the isolated impurity level E_{CFR} (see Fig. 6). The two latter quantities are measured in units Δ_0 meaning that the kinematic exchange and, hence, the Curie temperature is maximal for any given value of x when the impurity band is half filled, i.e., $\varepsilon_F = E_{CFR}^0$. At $x = 0.05$ the kinematic exchange $\overline{\Delta}$ may be about 0.14eV (if we assume that $\Delta_0 = 1\text{eV}$). The angular momentum $J = 2$ for the d^4 state of the Mn impurity in GaN, hence $T_C = \overline{\Delta}/k_B$, and we find that the value of the Curie temperature varies from a few hundred K for $x = 0.01$ and may exceed 1000K at $x = 0.05$.

It is worth mentioning that by choosing the localization radius so small, $\kappa^{-1} \approx d_0$, we have actually found a lower bound for $\overline{\Delta}$. At larger values of the localization radius, we obtain a similar dependence of the exchange energy $\overline{\Delta}$ on the Mn content and the Fermi energy position, however the absolute value of $\overline{\Delta}$ may become essentially larger, e.g. ~ 0.3 for $\kappa^{-1} \approx 2d_0$ in the maximum (see Fig. 7) meaning that the Curie temperature may become as high as several thousands K.

We should emphasize here again that the averaging procedure used to obtain the results in Figs. 5 and 6 works well only when the Fermi energy is close to the impurity level E_{CFR}^0 (zero on the Fermi energy axis). Far from this region one should apply the percolation approach proposed in Ref. 62. Then the effective kinematic exchange in this range may become smaller than shown in the figures, however the behavior does not change qualitatively, and certainly remains correct also quantitatively for ε_F close to E_{CFR}^0 .

To conclude this section, we have found that the optimum n -doping level for FM alignment of Mn spins corresponds approximately to half-filled impurity band, and one may well expect really high temperature magnetism in this case. The Curie temperature of $T_C = 940\text{K}$, reported in Ref.¹⁰, lies well within the range of values shown in Figs. 5 and 6. Unfortunately the lack of information on the impurity concentration and position of the Fermi level does not allow us to make a more detail comparison with the experiment.

V. CONCLUDING REMARKS

According to the general theory of magnetic interactions, the kinematic exchange between localized impurity spins embedded in a semiconductor host with covalent chemical bonding⁶³ is a generic property of the two-impurity cluster. We constructed such a cluster which was based on an ab initio knowledge about the electronic structure of isolated Mn impurity in a III-V semiconductor. After some simplifications this approach led us to a microscopic Hamiltonian similar to a two-center Anderson model.^{49,50} That model was developed for metallic hosts, whereas we consider a semiconductor host. The model allows for analytical solutions, and the final equation (23) for T_C with the effective coupling constant (18) should be compared with the phenomenological mean-field equation^{22,64}

$$T_C = \frac{4xS(S+1)J_{pd}^2}{3a} \frac{\chi_h}{(g\mu_B)^2} \quad (32)$$

where a is the lattice constant, J_{pd} is the phenomenological pd -exchange constant, χ_h is the magnetic susceptibility of holes in the valence band. In principle, Eq. (23) and Eq.

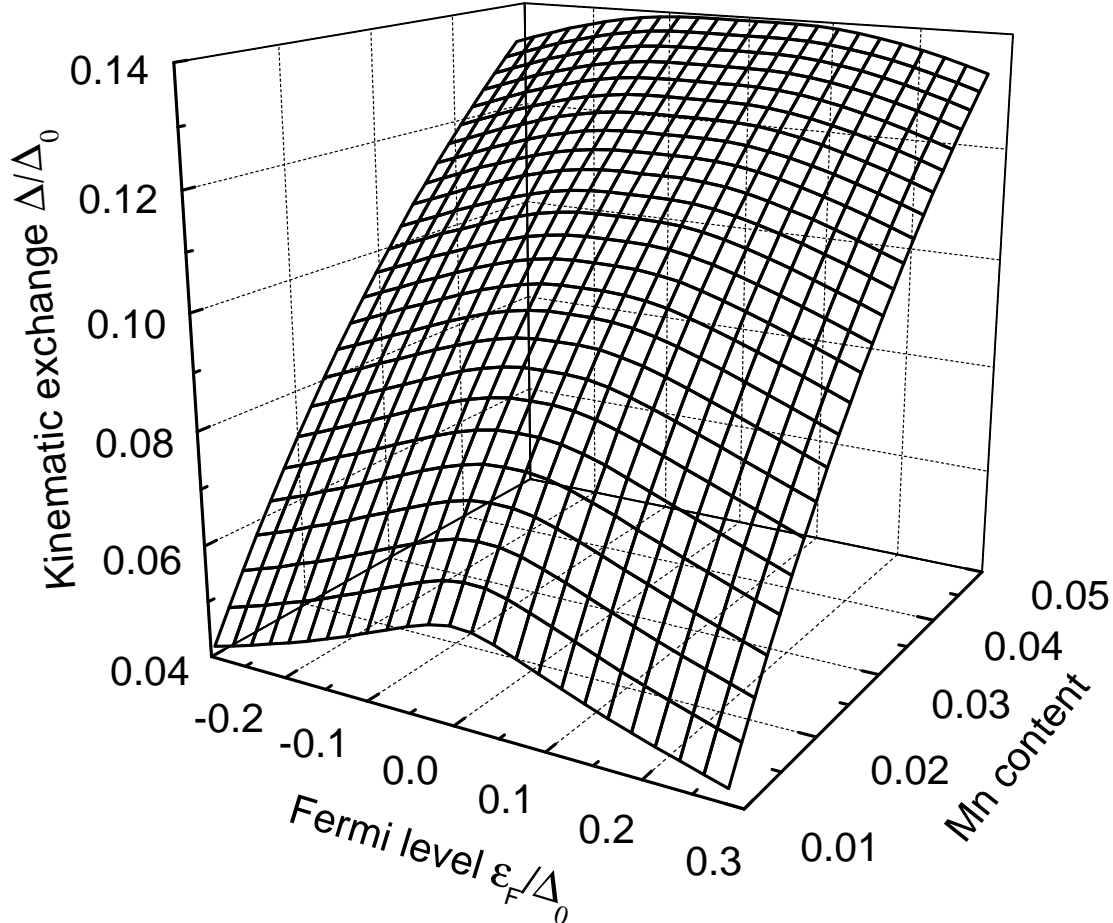


FIG. 6: Dependence of the kinematic exchange, measured in units of Δ_0 on the Mn content (x), and on the position of the Fermi energy relative to the level E_{CFR} of an isolated Mn impurity. We took $\kappa^{-1} = d_0$.

(32) consist of similar ingredients. It is natural to assume that J_{pd} in the phenomenological model stems from the hybridization. Then it may be derived in the Anderson-type model by means of the usual Schrieffer-Wolff transformation, so that $J_{pd} \sim V^2/(\varepsilon_F - E_d)$. Looking at Eq. (18) one can easily discern corresponding contributions, which in fact were proposed for dilute magnets four decades ago.⁶⁵ The second fraction in Eq. (32) is proportional to m^*k_F , i.e. to the Fermi momentum of holes in the valence band. *Unlike* the phenomenological model, which deals with localized spins and free holes near the top of the valence band, our model takes into account the change in the density of hole states (and therefore in their magnetic response) due to resonance scattering and impurity band formation. One of the results of this change is a more complicated dependence of the magnetic coupling on the Mn content x than the linear law predicted by Eq. (32). Another improvement of the mean-field theory taken into account in Eq. (23) is a more refined de-

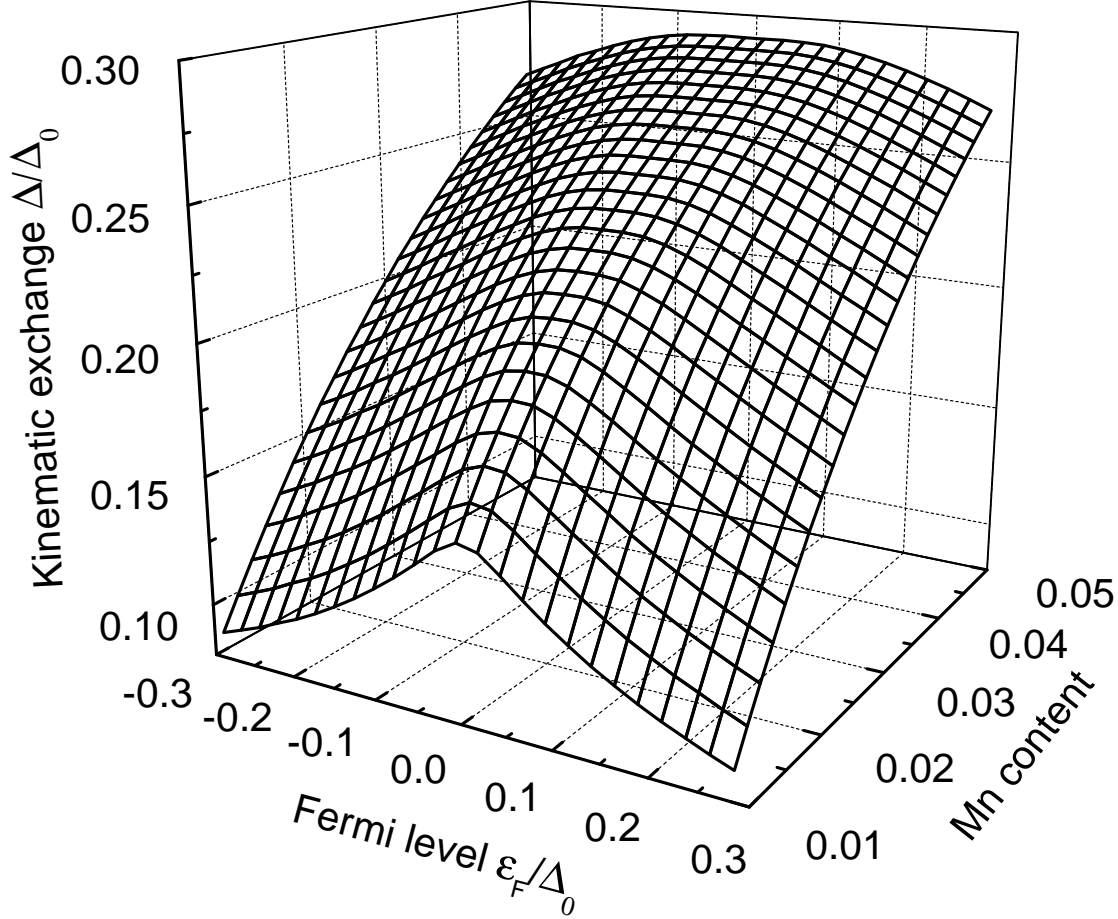


FIG. 7: The same as Fig. 6 but now for $\kappa^{-1} = 2d_0$.

scription of the impurity magnetic moment. The actual moment J arises as a vector sum of the moments of the d-electrons and the bound p-hole, One should emphasize that at a high enough concentration all mean-field descriptions fail because the alloy approaches the instability region and the Mn distribution becomes strongly inhomogeneous. In the case of $\text{Ga}_{1-x}\text{Mn}_x\text{As}$ this is, apparently, the region of $x > 0.07$.

Next, one should discuss the relation between our approach and the so called "ab initio" numerical calculations by means of the local-density functional method.^{29,30} Doping by Mn atoms is modelled in these calculations by means of a finite-size cluster of a GaAs or GaN host with one or several atoms replaced by Mn. Then periodic structures are constructed from magnetic clusters ("supercells") and the electronic bands in these artificial objects are calculated in the local-spin-density approximations (LSDA). So, the starting point in our approach and the LSDA calculations is the same. No wonder that the positions of CFR and DBH levels in these calculations are in good agreement with those used in our model, based on previous single impurity calculations.^{33,34} However, a direct comparison of the two procedures, as far as the magnetic properties are concerned, is somewhat

problematic. The self-consistent LSDA method results *by construction* only in a Stoner-like itinerant magnetism. Therefore, magnetic states are discussed in Refs. 29,30 in terms of exchange splitting and majority/minority spin subbands. It is difficult to discern the genuine kinematic double exchange in this type of calculations.

To overcome this difficulty, Sanvito *et al*²⁹ tried to fit their LSDA calculation by a free-electron model with an effective hole mass m^* and uniformly distributed impurities described by a model square potential containing spin-independent and exchange components ($W(r)$ and $J(r)$, respectively). Such separation is purely phenomenological. It ignores the resonance origin of the exchange potential. Besides, short-range impurity scattering cannot be described in the effective mass approximation.⁴⁵ Nevertheless, the estimate of the magnetic component $|J| = 1.05$ eV is in a good agreement with the corresponding parameter of our theory $\bar{z}V^2/E_{CFR} = 1.034$ eV for the parameters used in the fitting of Fig. 3 (the value of $W = 0.027$ eV is irrelevant because of the above mentioned effective mass approximation). One should emphasize, however, that the double-exchange coupling in our model is determined not by this parameter, but by the integral ΔE_{FM} (18), and this difference is in fact the benchmark for the discussion of the differences between the indirect pd exchange of Vonsovskii-Zener type⁶⁶ and the kinematic double exchange.³⁶

A simplified picture of the valence band structure used in our model (single heavy-hole band with semielliptic density of states) allowed us to describe the dependence $T_C(x, p)$ using a minimal number of fitting parameters. We have seen that a good quantitative agreement between theory and experiment could be achieved even with this very restricted set of parameters. With the help of a more realistic energy band scheme (e.g. by taking the light hole band into account), the restrictive symmetry of the density of states would be removed, and the fitting procedure would become more flexible. We intentionally imposed such severe restrictions on the model to demonstrate its explanatory capabilities. The above limitations will be lifted in future studies.

Further progress in the theoretical description of ferromagnetism in Mn-doped semiconductors is intimately related to the progress in sample preparation and characterization. At present more or less detailed data on $T_C(x, p)$ in p -type (Ga,Mn)As are available, and we succeeded in a quantitative description of these data within our model (Section III). We expect that the same approach is applicable to p -type (Ga,Mn)P, but the scanty experimental data do not allow us to check this expectation. As for (Ga,Mn)N, the accumulation of experimental data is in progress, and the most actual task is to reveal distinctions between p and n type magnetic alloys. Recent experimental data⁶⁷ confirm existence of magnetic order in n -(Ga,Mn)N, although the experimental state-of-the-art is far from providing trustworthy $T_c(x)$ curves for theoretical fitting. According to our theory, FM order is expected both in p - and n -type samples, but the latter case demands a serious modification of the theory (Section IV) and a direct extrapolation of the semi-empirical formula (32) is questionable.

Another challenging question is the possibility of ferromagnetism in elemental semiconductors and II-VI compounds doped by Mn and, maybe, other magnetic ions and respective modification of the theory. One can mention the recent reports about magnetism in Ge doped by Mn⁶⁸ and ZnO doped by Mn and Fe⁶⁹. In the latter case one

deals with a wide-gap semiconductor, where magnetic isoelectronic impurities Mn^{2+} and Fe^{2+} replace Zn ions. The theory presented in Section IV seems to be applicable in this case. Transition metal ions in Ge are as a rule interstitial impurities sometimes involved in formation of complex defects^{33,34,52}, so the existing theoretical approaches should be modified for this case. The most important conclusion from our study is that the electronic structure of an isolated magnetic impurity in the host material is the key to understanding its behavior in concentrated magnetic alloys.

Acknowledgments

This work was supported by the Flemish Science Foundation (FWO-VI), the Belgian Inter-University Attraction Poles (IUAP), the "Onderzoeksraad van de Universiteit Antwerpen" (GOA) and the Israeli Physical Society. VF and KK are grateful to Max-Planck Institute for Complex Systems (Dresden) for partial support and hospitality. VAI is grateful to Grenoble High Magnetic Field Laboratory (Centre National de la Recherche Scientifique and the Max-Planck Gesellschaft: CNRS-MPI)(Grenoble) for support and hospitality. Authors acknowledge useful and fruitful discussions with J. Cibert, K.W. Edmonds, B. Gallagher, H. Hori, Y.H. Jeong, T. Jungwirth, I. Ya. Korenblit, C. Lacroix, A. MacDonald, H. Mariette, S. Sonoda

APPENDIX A: ENERGY SPECTRUM OF TWO COUPLED IMPURITIES

The system of four Dyson equations for the d -electron Green functions $G_{dii'}^\sigma$ (i, i') has the following form within the Hartree approximation:

$$G_{dii'}^\sigma(\varepsilon) = g_{d\sigma}(\varepsilon) \left(\delta_{ii'} + \sum_{\mathbf{p}\mathbf{p}'} \sum_{j=1,2} V_{\mathbf{p}d} V_{\mathbf{p}'d}^* e^{-i\mathbf{p}\cdot\mathbf{R}_i} G_{\mathbf{p}\mathbf{p}'}^\sigma e^{i\mathbf{p}'\cdot\mathbf{R}_l} G_{dj i'}^\sigma \right). \quad (\text{A1})$$

Here

$$g_{d\sigma}(\varepsilon) \delta_{ij} = (\varepsilon - E_d - U n_i^{-\sigma} + i\delta \text{sign}(\varepsilon - \mu))^{-1} \delta_{ij} \quad (\text{A2})$$

is the bare single site d -electron Green function for the $t_2\sigma$ electron centered at the ion i , taken in the Hartree approximation. μ is the chemical potential. The Green function for the band electrons can be found from the Dyson equation (a similar system of equations for two Anderson impurities in metal was analyzed in Ref. 50)

$$\overline{G}_{\mathbf{p}\mathbf{p}'}^\sigma(\varepsilon) = G_{\mathbf{p}\mathbf{p}'}^\sigma(\varepsilon) + \sum_{\mathbf{p}''\mathbf{p}'''ij} G_{\mathbf{p}\mathbf{p}''}^\sigma(\varepsilon) V_{\mathbf{p}''di} g_{d\sigma}(\varepsilon) V_{\mathbf{p}'''dj}^* \overline{G}_{\mathbf{p}''\mathbf{p}'}^\sigma(\varepsilon) e^{i(\mathbf{p}''\cdot\mathbf{R}_i - \mathbf{p}'''\cdot\mathbf{R}_j)}. \quad (\text{A3})$$

There are also impurity off-diagonal Green functions, which read

$$G_{di\mathbf{p}}^\sigma(\varepsilon) = g_{i\sigma}(\varepsilon) V_{\mathbf{p}''d}^* \overline{G}_{\mathbf{p}\mathbf{p}'}^\sigma(\varepsilon). \quad (\text{A4})$$

The Green function $G_{\mathbf{p}\mathbf{p}'}^\sigma$ describes the spectrum of the valence band electrons modified by the two-impurity short-range potential scattering. It satisfies the Dyson equation

$$G_{\mathbf{p}\mathbf{p}'}^\sigma(\varepsilon) = g_{\mathbf{p},\sigma}(\varepsilon)\delta_{\mathbf{p}\mathbf{p}'} + g_{\mathbf{p},\sigma}(\varepsilon) \sum_{\mathbf{p}''} W_{\mathbf{p}\mathbf{p}''} G_{\mathbf{p}''\mathbf{p}'}^\sigma(\varepsilon) \quad (\text{A5})$$

where

$$g_{\mathbf{p},\sigma}(\varepsilon) = (\varepsilon - \varepsilon_{\mathbf{p}} + i\delta\text{sign}(\varepsilon - \mu))^{-1}. \quad (\text{A6})$$

All the above equations give linear relations between the Green functions. We may rewrite equation (A5) using shorthand notations for the Green function matrices

$$\mathbf{G}_b = \mathbf{A} \cdot \mathbf{g}_b \quad (\text{A7})$$

where \mathbf{g}_b stands for the diagonal matrix (A6). Equations (A1) and (A4) take the form

$$\mathbf{G} = \mathbf{B} \cdot \mathbf{g}_0 \quad (\text{A8})$$

where

$$\mathbf{g}_0 = \begin{pmatrix} \mathbf{G}_b & 0 \\ 0 & \mathbf{g}_d \end{pmatrix}.$$

with \mathbf{g}_d being a 2×2 matrix (A2). The explicit expressions for the matrices \mathbf{A} and \mathbf{B} can be readily found from the Dyson equations (A1), (A4), and (A5).

For further calculations we need determinants of the matrices \mathbf{A} and \mathbf{B} ,

$$\mathbf{Q}(\varepsilon) \equiv \det \mathbf{A} = \mathbf{q}(\varepsilon)^2 - W^2 L_{12}(\varepsilon) L_{21}(\varepsilon), \quad (\text{A9})$$

where

$$\mathbf{q}(\varepsilon) = 1 - W L_{11}(\varepsilon)$$

and

$$L_{ij} = \sum_{\mathbf{p}} g_p^0 e^{i\mathbf{p} \cdot (\mathbf{R}_i - \mathbf{R}_j)} \quad (\text{A10})$$

is the lattice Green function. We assume that $L_{11} = L_{22}$. The second determinant is

$$\mathbf{R} \equiv g_d^{-2}(\varepsilon) \det \mathbf{B} = [g_d^{-1}(\varepsilon) - V^2 M_{11}^\sigma(\varepsilon)]^2 - V^4 M_{12}^\sigma(\varepsilon) M_{21}^\sigma(\varepsilon). \quad (\text{A11})$$

Here

$$M_{11}^\sigma = \sum_{\mathbf{p}\mathbf{p}'} e^{-i(\mathbf{p}-\mathbf{p}') \cdot \mathbf{R}_1} G_{\mathbf{p}\mathbf{p}'}^\sigma = L_{11} + W\mathbf{Q}^{-1}[L_{11}^2 \mathbf{q} + L_{12} L_{21} \mathbf{q} + 2W L_{11} L_{12} L_{21}]. \quad (\text{A12})$$

M_{22}^σ is obtained from Eq. (A12) by exchanging indices 1 and 2, and

$$M_{12}^\sigma = \sum_{\mathbf{p}\mathbf{p}'} e^{-i\mathbf{p} \cdot \mathbf{R}_1 + i\mathbf{p}' \cdot \mathbf{R}_2} G_{\mathbf{p}\mathbf{p}'}^\sigma = L_{12} + W\mathbf{Q}^{-1}[L_{12} L_{11} \mathbf{q} + L_{21} L_{11} \mathbf{q} + W L_{21}^2 L_{12}]. \quad (\text{A13})$$

Till now the calculations were made neglecting the orbital degeneracy of the impurity d states and within the Hartree approximation. We can generalize these calculations using

the Hubbard I approximation for the d -electron Green functions (see, e.g., Ref. 51). We assume also that the three-fold degeneracy of the impurity t_{2g} is not lifted and the relevant physical quantities do not depend on the index μ enumerating these three states. The algebraic structure of the Dyson equation is still the same as in (A1). Then considering the interaction of two three-fold degenerate states belonging to the two impurities. This leads to the 6×6 matrix

$$\mathbf{B}'_{i\mu,j\mu'} = \begin{pmatrix} a & 0 & 0 & b & b & b \\ 0 & a & 0 & b & b & b \\ 0 & 0 & a & b & b & b \\ b & b & b & a & 0 & 0 \\ b & b & b & 0 & a & 0 \\ b & b & b & 0 & 0 & a \end{pmatrix} \quad (\text{A14})$$

where

$$a = g_d^{-1}(\varepsilon) - V^2 K M_{11}^\sigma(\varepsilon), \quad b = V^2 K M_{12}^\sigma(\varepsilon)$$

and $K = n_{d^5} + n_{d^4}$. n_{d^5} is the probability that the impurity d -shell is in the nondegenerate d^5 state, whereas n_{d^4} is the probability that the impurity d -shell is in one of the three degenerate d^4 states. Calculating now the determinant of the matrix (A14) one gets the equation

$$\mathbf{R} \equiv a^{-4} \det \mathbf{B}' = [g_d^{-1}(\varepsilon) - V^2 K M_{11}^\sigma(\varepsilon)]^2 - 9V^4 K^2 M_{12}^\sigma(\varepsilon) M_{21}^\sigma(\varepsilon). \quad (\text{A15})$$

which should be used instead of Eq. (A11).

The occupation numbers n_{d^5} and n_{d^4} for the Hubbard-like states obey a non-Fermi statistics, whose specific form in the case considered here is

$$n_{d^5} = \frac{f(E_{CFR} - \mu)}{3 - 2f(E_{CFR} - \mu)}, \quad n_{d^4} = \frac{1 - f(E_{CFR} - \mu)}{3 - 2f(E_{CFR} - \mu)} \quad (\text{A16})$$

If the chemical potential lies below the impurity level E_{CFR} of the fifth electron in the d -shell then the Fermi distribution $f(E_{CFR} - \mu)$ is zero at low temperatures and $n_{d^5} = 0$, $n_{d^4} = 1/3$, meaning that $K = 1/3$. If $E_{CFR} < \mu$ then $n_{d^5} = 1$, $n_{d^4} = 0$, and $K = 1$.

The energy (5) can be found using the general property of the Green functions, connecting their trace and determinant

$$\text{Tr } \mathbf{G}(\varepsilon) = \frac{d}{d\varepsilon} \ln \det \mathbf{G}(\varepsilon) \quad (\text{A17})$$

Then using Eqs. (A9) and (A11), (A17) allows one to rewrite Eq. (5) in the following form

$$\Delta E = \text{Im} \int_{-\infty}^{\infty} \frac{d\varepsilon}{2\pi} \varepsilon \frac{d}{d\varepsilon} [\ln \mathbf{R}^\sigma(\varepsilon) + \ln \mathbf{Q}^\sigma(\varepsilon)] = -\text{Im} \int_{-\infty}^{\infty} \frac{d\varepsilon}{2\pi} [\ln \mathbf{R}^\sigma(\varepsilon) + \ln \mathbf{Q}^\sigma(\varepsilon)]. \quad (\text{A18})$$

The functions \mathbf{R} and \mathbf{Q} depend on the combination $\varepsilon - i\text{sign}(\varepsilon - \mu)$, hence the integration contour in (A18) can be deformed in such a way as to embrace the cut from the band

states and all the poles due to the localized levels with the energies below the chemical potential μ , i.e. occupied states. Then equation (A18) transforms into (6).

Next we consider a property of Eq. (A18), which will simplify the calculation of the energy and provides a better intuition to the results. Our model includes all the levels belonging to the valence band with the addition of the impurity d -levels, which interact with the band levels. Let us assume that at zero temperature the chemical potential lies higher than all these levels, meaning that they are all occupied. Then the total energy of the system is

$$E_{tot} = \text{Tr} \hat{H}. \quad (\text{A19})$$

In order to calculate this trace, we may represent the operator \hat{H} in matrix form using the noninteracting band states with the addition of the atomic d -functions as the basis. Then the hybridization matrix elements will appear only in the off-diagonal positions of this matrix, which do not influence the result. The conclusion is that the energy E_{tot} does not depend on the value of the hybridization.

The potential scattering, $W_{\mathbf{pp}}$, contributes to the diagonal elements of the Hamiltonian and may influence the value of E_{tot} . However, we are interested here only in the indirect exchange between the impurities. It can be found if we consider the energy $\Delta E(R_{ij})$ and subtract from it the energy corresponding to two noninteracting impurities,

$$\Delta E_{ex} = -\frac{1}{\pi} \text{Im} \int_{\varepsilon_{hb}}^{\mu} d\varepsilon \left[\ln \frac{R^\sigma(\varepsilon)}{R_0^\sigma(\varepsilon)} + \ln \frac{Q^\sigma(\varepsilon)}{Q_0^\sigma(\varepsilon)} \right] + \Delta E_{loc}(\varepsilon < \mu). \quad (\text{A20})$$

where $Q_0^\sigma(\varepsilon)$ and $R_0^\sigma(\varepsilon)$ are obtained from (A9) and (A11) under the assumption that $L_{12} = L_{21} = 0$. $\Delta E_{loc}(\varepsilon < \mu)$ is the corresponding change of the energies of the occupied localized levels. Now we may conclude that the sum (A20) over all occupied states is equal to the same sum over all empty states, but with the opposite sign. Hence,

$$\Delta E_{ex} = \frac{1}{\pi} \text{Im} \int_{\mu}^{\varepsilon_{ht}} d\varepsilon \left[\ln \frac{R^\sigma(\varepsilon)}{R_0^\sigma(\varepsilon)} + \ln \frac{Q^\sigma(\varepsilon)}{Q_0^\sigma(\varepsilon)} \right] - \Delta E_{loc}(\varepsilon > \mu). \quad (\text{A21})$$

Here $\Delta E_{loc}(\varepsilon > \mu)$ includes the empty localized levels (if any) lying above the chemical potential. These levels appear due to the combined action of both potential (W) and resonance (V) scattering mechanisms. Formally they can be found as zeros of the determinant R (A11).

To find the contribution of the localized states to the magnetic energy one should simply calculate the level positions modified by the effective inter-impurity exchange due to hopping via empty states and their occupation. We consider here two limiting cases.

First, we estimate the contribution of CFR levels, if they happen to lie within the forbidden energy gap. It means that we may expand the function $R(\varepsilon)$ close to the energy $E_{CFR\sigma}^0$ of the isolated CFR level determined by the equation

$$E_{CFR}^0 = E_d + KV^2 P_{11}(E_{CFR}^0), \quad (\text{A22})$$

which describes the TM d -levels renormalized by their hybridization with the hh band. Indirect inter-impurity hopping results in splitting of two-impurity states and a shift of

localized states relative to the hh band. These levels lie in the discrete part of the spectrum, where the imaginary part of the Green function (9) $\Gamma_{ij} = 0$. Neglecting potential scattering, we obtain the equation

$$\mathbf{R} = [\varepsilon - E_d - KV^2 P_{11}^\sigma(\varepsilon)][\varepsilon - E_d - KV^2 P_{22}^\sigma(\varepsilon)] - 9K^2 V^4 P_{12}^\sigma(\varepsilon) P_{21}^\sigma(\varepsilon) = 0. \quad (\text{A23})$$

for the two-impurity poles in the energy gap. The solution of Eq. (A23) is looked for in the form $E_{CFR} = E_{CFR}^0 + \delta E_{CFR}$. Now we expand the function $\mathbf{R}(E_{CFR}^0 + \delta E_{CFR})$ up to the second order terms with respect to δE_{CFR} and arrive at Eq. (11).

Second, we consider the case when the DBH levels lie in the forbidden energy gap. Then the potential scattering W is the leading cause of the creation of the deep level. The energy of an isolated DBH level corresponds to a zero of the function

$$\mathbf{q}(E_{DBH}^0) = 1 - WP_{11}(E_{DBH}^0) = 0.$$

Then we look for zeros of the function $\mathbf{R}(\varepsilon)$ at the energy $E_{DBH} = E_{DBH}^0 + \delta E_{DBH}$. Accounting for the fact that both functions \mathbf{q} and \mathbf{Q} are small in the vicinity of the energy E_{DBH}^0 the equation $\mathbf{R} = 0$ can be approximately rewritten in the form

$$\left\{ \mathbf{q}^2 - W^2 P_{12}^2 - \frac{KV^2}{\Delta E} W [P_{11}^2 \mathbf{q} + P_{12}^2 \mathbf{q} + 2WP_{11} P_{12}^2] \right\}^2 = \frac{9K^2 V^4}{\Delta E^2} \{ P_{12} + W [2P_{12} P_{11} \mathbf{q} + WP_{12}^2] \}^2 \quad (\text{A24})$$

with $\Delta E = E_{DBH}^0 - E_d - V^2 P_{11}$. All the functions P_{ij} are now calculated at $\varepsilon = E_{DBH}^0$. We first neglect the r.h.s term in Eq. (A24) and solve the quadratic equation

$$\mathbf{q}^2 - \frac{KV^2}{\Delta E} W [P_{11}^2 + P_{12}^2] \mathbf{q} - W^2 P_{12}^2 - \frac{2KV^2 W^2}{\Delta E} P_{11} P_{12}^2 = 0. \quad (\text{A25})$$

From here we obtain Eq. (15) for the energy shifts due to hopping between the two degenerate DBH levels.

When both these levels are empty we obtain a contribution to the kinematic exchange by summing these two energies, extracting from them the part due to the hybridization with the impurity d-states, and changing the sign in the hole representation,

$$\Delta E_{DBH,ex} = \frac{KV^2 P_{12}^2}{\Delta E P_{11}}. \quad (\text{A26})$$

Accounting for the rhs of Eq. (A24) will result in higher order corrections, which can be neglected.

* Till December 2002 in Departement Natuurkunde, Universiteit Antwerpen

Electronic address: fleurov@post.tau.ac.il

- ¹ M. Ilegems, R. Dingle, and L.W. Rupp (Jr.), *J. Appl. Phys.* **46**, 3059 (1975); D.G. Andrianov, V.V. Karataev, G.V. Lazarev, Yu.B. Muravlev, and A.S. Savel'ev, *Sov. Phys. Semicond.* **11**, 738 (1977); T. Hayashi, Y. Hashimoto, S. Katsumoto, and Y. Iye, *Appl. Phys. Lett.* **78**, 1691 (2001).
- ² F. Matsukura, H. Ohno, A. Shen, and Y. Sugawara, *Phys. Rev. B* **57**, R2037 (1998).
- ³ J. M. Kikkawa and A. D. Awschalom, *Nature (London)* **397**, 139 (1998).
- ⁴ H. Ohno, H. Munekata, T. Penney, S. von Molnár, and L. L. Chang, *Phys. Rev. Lett.* **68**, 2664 (1992).
- ⁵ H. Ohno, *J. Magn. Magn. Mater.* **200**, 110 (1999); *Science* **281**, 951 (1998).
- ⁶ K. W. Edmonds, K. Y. Wang, R. P. Campion, A. C. Neumann, N. R. S. Farley, B. L. Gallagher, and C. T. Foxon, *Appl. Phys. Lett.* **81**, 4991 (2002).
- ⁷ I. Kuryliszyn, T. Wojtowicz, X. Liu, J. K. Furdyna, W. Dobrowolski, J.-M. Broto, M. Goiran, O. Portugal, H. Rakoto, B. I. Raquet, *Acta Phys. Pol. A* **102**, 659 (2002).
- ⁸ K. C. Ku, S. J. Potashnik, R. F. Wang, S. H. Chun, P. Schiffer, and N. Samarth, M. J. Seong and A. Mascarenhas, E. Johnston-Halperin, R. C. Myers, A. C. Gossard, and D. D. Awschalom *Appl. Phys. Lett.* **82**, 2302 (2003); K.W. Edmonds, P. Boguslawski, K.Y. Wang, R.P. Campion, N.R.S. Farley, B.L. Gallagher, C.T. Foxon, M. Sawicki, T. Dietl, M.B. Nardelli, and J. Bernholc cond-mat/0307140.
- ⁹ B. Gallagher, CECAM Workshop: "Diluted Magnetic Semiconductors", June 12-14 2003, Lyon.
- ¹⁰ S. Sonoda, S. Shimizu, T. Sasaki, Y. Yamamoto, and H. Hori, *J. Appl. Phys.* **91**, 7911 (2002).
- ¹¹ M. L. Reed, N. A. El-Masry, H. H. Stadelmaier, M. K. Ritums, M. J. Reed, C. A. Parker, J. C. Roberts, and S. M. Bedair, *Appl. Phys. Lett.* **79**, 3473 (2001). N. Theodoropoulou, A. F. Hebard, M. E. Overberg, S. N. G. Chu, and R. G. Wilson, *Appl. Phys. Lett.* **78**, 3475 (2001); M. E. Overberg, C. R. Abernathy, S. J. Pearton, N. A. Theodoropoulou, K. T. McCarthy, and A. F. Hebard, *Appl. Phys. Lett.* **79**, 1312 (2001).
- ¹² S. A. Crooker, D. A. Tulchinsky, J. Levy, D. D. Awschalom, R. Garcia, N. Samarth, *Phys. Rev. Lett.* **75**, 505 (1995).
- ¹³ D. P. Di Vincenzo, *Science* **270**, 255 (1995).
- ¹⁴ H. Ohno, D. Chiba, F. Matsukura, T. Omiya, E. Abe, T. Dietl, Y. Ohno, and K. Ohtani, *Nature (London)* **408**, 944 (2000).

- ¹⁵ A. Oiwa, Y. Mitsumori, R. Moriya, T. Slupinski, and H. Munekata, Phys. Rev. Lett. **88**, 137202 (2002).
- ¹⁶ M. Tanaka and Y. Higo, Phys. Rev. Lett. **87**, 026602 (2001).
- ¹⁷ J. König, J. Schlieman, T. Jungwirth, and A. H. MacDonald, in "Electronic Structure and Magnetism of Complex Materials" (Springer Verlag, Berlin, 2002).
- ¹⁸ H. Ohno, D. Chiba, F. Matsukara, T. Omiyama, E. Abe, T. Dietl, Y. Ohno, and K. Ohtani, Nature (London) **408**, 944 (2000).
- ¹⁹ R. K. Kawakami, E. Johnston-Halperin, L. F. Chen, M. Hanson, N. Guébels, J.S. Speck, A. C. Gossard, and D. D. Awschalom, Appl. Phys. Lett. **77**, 2379 (2000).
- ²⁰ B. Lee, T. Jungwirth, and A.H. MacDonald, Phys. Rev. B **65**, 193311 (2002).
- ²¹ H. Ohno, A. Shen, F. Matsukara, O. Oiwa, A. Endo, S. Katsumoto, and Y. Iye, Appl. Phys. Lett. **69**, 363 (1996).
- ²² T. Dietl, H. Ohno, F. Matsukura, J. Cibert, and D. Ferrand, Science **287**, 139 (1998).
- ²³ T. Dietl, H. Ohno, and F. Matsukura, Phys. Rev. B **63**, 195205 (2001).
- ²⁴ T. Dietl, F. Matsukura, and H. Ohno, Phys. Rev. B **66**, 033203 (2002).
- ²⁵ M. Berciu and R. N. Bhatt, Phys. Rev. Lett. **87**, 107203, 2001.
- ²⁶ Yu. G. Semenov and S.M. Ryabchenko, Low Temp. Phys. **26**, 886 (2000) [Fizika Nizkikh Temperatur **26**, 1197 (2000)].
- ²⁷ V. K. Dugaev, V.I. Litvinov, J. Barnaś, and M. Vieira, Phys. Rev. B **67**, 033201 (2003).
- ²⁸ J. Inoue, S. Nonoyama, and H. Itoh, Phys. Rev. Lett. **85**, 4610 (2000); Physica E **10**, 170 (2001).
- ²⁹ S. Sanvito, P. Ordejón, and N.A. Hill, Phys. Rev. B **63**, 165206 (2001).
- ³⁰ K. Sato and H. Katayama-Yoshida, Jpn. J. Appl. Phys. **40**, L485 (2001); P. Mahadevan and A. Zunger, "Electronic structure and ferromagnetism of 3d transition metal impurities in GaAs" (preprint); L. Kronik, M. Jain, and J. R. Chelikowsky, Phys. Rev. B **66**, 041203(R) (2002); M. van Schilfgaarde and O. N. Mryasov, Phys. Rev. B **63**, 233205 (2001); E. Kulatov, H. Nakayama, H. Mariette, H. Ohta, and Y. A. Uspenskii, Phys. Rev. B **66**, 045203 (2002).
- ³¹ V. N. Fleurov and K. A. Kikoin, J. Phys. C: Solid State Phys. **9**, 1673 (1976).
- ³² F. D. M. Haldane and P. W. Anderson, Phys. Rev. B **13**, 2553 (1976).
- ³³ K. A. Kikoin and V. N. Fleurov, "Transition Metal Impurities in Semiconductors", (World Scientific, Singapore, 1994).

- ³⁴ A. Zunger, in *Solid State Physics*, Ed. by H. Ehrenreich and D. Turnbull (Academic, Orlando, 1986) Vol. **39**, p. 276.
- ³⁵ P. M. Krstajić, V. A. Ivanov, F. M. Peeters, V. Fleurov, and K. Kikoin, *Europhys. Lett.* **61**, 235 (2003).
- ³⁶ C. Zener, *Phys. Rev.* **82**, 403 (1951).
- ³⁷ J. Schneider, U. Kaufmann, W. Wilkening, M. Baeumler, and F. Köhl, *Phys. Rev. Lett.* **59**, 240 (1987).
- ³⁸ M. Linnarsson, E. Janzen, B. Monemar, M. Kleverman, and A. Thilderkvist, *Phys. Rev. B* **55**, 6938 (1997).
- ³⁹ J. Szczytko, A. Twardowski, K. Swiatek, M. Palczewska, M. Tanaka, and T. Hayashi, K. Ando, *Phys. Rev. B* **60**, 8304 (1999).
- ⁴⁰ Y. Nagai, T. Kunimoto, K. Nagasaka, H. Nojiri, M. Motokawa, F. Matsukura, T. Dietl, and H. Ohno, *Jpn. J. Appl. Phys.* **40**, 6231 (2001).
- ⁴¹ K. A. Kikoin and V. N. Fleurov, *J. Phys. C: Solid State Phys.* **10**, 4295 (1977).
- ⁴² L. A. Hemstreet, *Phys. Rev. B* **22**, 4590 (1980).
- ⁴³ G. Picoli, A. Chomette, and M. Lannoo, *Phys. Rev. B* **30**, 7138 (1984).
- ⁴⁴ V. A. Singh and A. Zunger, *Phys. Rev. B* **31**, 3729 (1985).
- ⁴⁵ V. N. Fleurov and K. A. Kikoin, *J. Phys. C: Solid State Phys.* **19**, 887 (1986).
- ⁴⁶ K. A. Kikoin and V. N. Fleurov, *J. Phys. C: Solid State Phys.* **17**, 2357 (1984).
- ⁴⁷ T. Graf, M. Gjukic, L. Görgens, O. Ambacher, M. S. Brandt, and M. Stutzmann, *Appl. Phys. Lett.* **81**, 5159 (2002).
- ⁴⁸ P. W. Anderson, *Phys. Rev.* **124**, 41 (1961).
- ⁴⁹ S. Alexander and P. W. Anderson, *Phys. Rev.* **133**, A1594 (1964).
- ⁵⁰ B. Caroli, *J. Phys. Chem. Solids* **28**, 1427 (1967).
- ⁵¹ K. A. Kikoin and V. N. Fleurov, *Zh. Eksp. Teor. Fiz.* **77**, 1062 (1979) [*JETP* **50**, 535 (1979)].
- ⁵² *Data in Science and Technology - Semiconductors: Group IV Elements and III-V Compounds*, edited by O. Madelung (Springer-Verlag, Berlin, 1991).
- ⁵³ K. W. Edmonds, K. Y. Wang, R. P. Champion, A. C. Neumann, C. T. Foxon, B. L. Gallagher, and P. C. Main, *Appl. Phys. Lett.* **81**, 3010 (2002).
- ⁵⁴ N. Theodoropoulou, A. F. Hebard, M. E. Overberg, C. R. Abernathy, S. J. Pearton, S. N. G. Chu, and R. G. Wilson, *Phys. Rev. Lett.* **89**, 107203 (2002).

- ⁵⁵ V. Barzykin, arXiv:cond-mat/0311114.
- ⁵⁶ H. Asklund, L. Ilver, J. Kanski, J. Sadowski, and R. Mathieu Phys. Rev. B **66**, 115319 (2002).
- ⁵⁷ H. Ohno and F. Matsukura, Solid State Commun. **117**, 179 (2001).
- ⁵⁸ K. M. Yu, W. Walukiewicz, T. Wojtowicz, W. L. Lim, X. Liu, Y. Sasaki, M. Dobrowolska, and J. K. Furdyna, Appl. Phys. Lett. **81**, 5 (2002).
- ⁵⁹ T. Jungwirth, J. König, J. Sinova, J. Kucera, and A.H. MacDonald, Phys. Rev. B **66**, 012402 (2002).
- ⁶⁰ I. Ya. Korenblit and E. F. Shender, Zh. Exp. Teor. Fiz. **62**, 1949 (1972) [Sov. Phys. - JETP **35**, 1017]; S. L. Ginzburg, I. Ya. Korenblit, I. Y. Shender, Zh. Exp. Teor. Fiz. **64**, 2255 (1973) [Sov. Phys. JETP **37**, 1141].
- ⁶¹ I. Ya. Korenblit and E.F. Shender, Usp. Fiz. Nauk **126**, 233 (1978) [Sov. Phys. - Uspekhi **21**, 832 (1978)].
- ⁶² I. Ya. Korenblit, E. F. Shender, and B. I. Shklovskii, Phys. Lett. **46A**, 275 (1973).
- ⁶³ P. W. Anderson, Phys. Rev. **79**, 350 (1950); J. B. Goodenough, *Magnetism and Chemical Bond* (Interscience Publ., N. Y., 1963).
- ⁶⁴ T. Jungwirth, W. A. Atkinson, B. H. Lee, and A. H. MacDonald, Phys. Rev. B **59**, 9818 (1999).
- ⁶⁵ A.A. Abrikosov and L.P. Gorkov, Zh. Eksp. Teor. Fiz. **43**, 2230 (1962) [Sov. Phys. - JETP, **16**, 1575 (1963)].
- ⁶⁶ S. V. Vonsovskii, Zh. Exp. Teor. Fiz. **16**, 981 (1946); C. Zener, Phys. Rev. **81**, 440 (1951).
- ⁶⁷ P.P. Chen, H. Makino, J.J. Kim, and T. Chao, J. Cryst. Growth **251**, 331 (2003); R. Giraud, S. Kuroda, S. Marcet, E. Bellet-Amarlic, X. Biquard, B. Barbara, D. Fruchart, J. Cibert, and H. Mariette, Europhys. Lett., submitted
- ⁶⁸ S. Cho, S. Choi, S.-C. Hong, Y. Kim, J. B. Ketterson, B.-J. Kim, Y. C. Kim, and J.-H. Jung, Phys. Rev. B **66**, 033303 (2002); A. Stroppa, S. Picozzi, and A. Continenza, A. J. Freeman, PRB **68**, 155203 (2003); Y. D. Park, A. T. Hanbicki, S. C. Erwin, C. S. Hellberg, J. M. Sullivan, J. E. Mattson, T. F. Ambrose, and A. Wilson, Science **295**, 651 (2002); F. Tsui, L. He, L. Ma, A. Tkachuk, Y. S. Chu, K. Nakajima, and T. Chikyow, Phys.Rev.Lett. **91**, 177203 (2003).
- ⁶⁹ K. Ueda, H. Tabata, and T. Kawai, Appl. Phys. Lett. **79**, 988 (2001); D. P. Norton, S. J. Pearton, A. F. Hebard, N. Theodoropoulou, L. A. Boatner, R. G. Wilson, Appl. Phys. Lett.

82, 239 (2003).